Article

Renormalization in Quantum Brain Dynamics

Akihiro Nishiyama [1,*] , **Shigenori Tanaka** [1] **and Jack A. Tuszynski** [2,3,4]

1   Graduate School of System Informatics, Kobe University, 1-1 Rokkodai, Nada-ku, Kobe 657-8501, Japan
2   Department of Oncology, Cross Cancer Institute, University of Alberta, Edmonton, AB T6G 1Z2, Canada
3   Department of Physics, University of Alberta, Edmonton, AB T6G 2J1, Canada
4   Department of Mechanical and Aerospace Engineering, Corso Duca degli Abruzzi, 24, Politecnico di Torino, 10129 Turin, Italy
*   Correspondence: anishiyama@people.kobe-u.ac.jp

Abstract: We show renormalization in Quantum Brain Dynamics (QBD) in $3 + 1$ dimensions, namely Quantum Electrodynamics with water rotational dipole fields. First, we introduce the Lagrangian density for QBD involving terms of water rotational dipole fields, photon fields and their interactions. Next, we show Feynman diagrams with 1-loop self-energy and vertex function in dipole coupling expansion in QBD. The counter-terms are derived from the coupling expansion of the water dipole moment. Our approach will be applied to numerical simulations of Kadanoff–Baym equations for water dipoles and photons to describe the breakdown of the rotational symmetry of dipoles, namely memory formation processes. It will also be extended to the renormalization group method for QBD with running parameters in multi-scales.

1. Introduction

The human brain is one of the most complex and poorly understood biological structures studied by science. This is especially true regarding the molecular mechanisms of how the human brain works, especially its information processing and memory encoding functions. While much is known about the architecture of brain cells and their individual activities in terms of the action potential, ion channels and ionic currents [1], much less is known about such issues as where our memories are stored or which molecular mechanisms are involved in information processing and higher cognitive functions. Much has been speculated recently about the possibility of at least some cognitive functions requiring the operation at a level of quantum physics or even quantum field theory [2,3]. Experimental determination or even corroboration of such ideas is currently beginning to be achievable in view of the modern experimental methods and instrumentation available to researchers [4].

Electromagnetic (EM) *field* theories of consciousness propose that consciousness results when a brain produces an electromagnetic field with specific characteristics. Pockett [5] and McFadden [6] have proposed EM field theories; Some electromagnetic theories are also quantum mind theories of consciousness; examples include the Quantum Brain Dynamics (QBD) approaches of Jibu and Yasue [7] and Vitiello [8], who proposed a quantum field theory explanation of how memory is created. In general, quantum mind theories other than these QBD approaches do not treat consciousness as an electromagnetic phenomenon. The basis for McFadden and Pockett's CEMI theory is the neuron's firing, which generates an action potential that is then the trigger for a postsynaptic potential in the neighboring neuron. Moreover, this ionic current also perturbs the surrounding electromagnetic field. McFadden has proposed that the brain's electromagnetic field represents an information-rich signal in the neurons. This hypothesis is supported by demonstrated effects of weak EM

fields on the activity of the human brain, e.g., in well-documented reports on the so-called photobiomodulation [9,10]. McFadden has proposed that the digital information processed by neurons is integrated to create a conscious electromagnetic information (CEMI) field in the brain. Moreover, experiments performed by Christof Koch and his team demonstrated that external EM fields simulate the brain's endogenous EM fields and influence neuronal firing patterns [11].

Following on from the seminal work of Stuart, Umezawa and Takahashi [12], the present authors have recently provided fundamental results for the realistic development of a quantum field theory of the dynamics of the brain that include hierarchical organization of the neurons, the microscopic intraneuronal structure, including the cytoskeleton and ordered water, as well as nonlinear dynamics [13–15]. The methodology adopted includes an open system, non-equilibrium and nonlinear approach to the field theoretic description that is seen as the most simplified adequate representation of Quantum Brain Dynamics. We have shown in this work how decoherence can be properly described within this framework and hence how to minimize it, which is a major issue in applying quantum concepts to the functioning of the brain. Although there are objections to the methodology adopting quantum coherence in brain dynamics represented by [16], we find quantum effects in magneto-reception, olfaction and photosynthesis in the context of quantum biology [17]. Moreover, a recent experimental result suggests that our brain adopts quantum entanglement by studying zero quantum coherence [18]. Considering recent experimental suggestions, it might be rash to exclude quantum effects in brain dynamics.

Quantum Brain Dynamics (QBD) represents one of the hypotheses expected to describe memory in the brain [19–21]. It originated with the monumental work by Ricciardi and Umezawa in 1967 [22]. They adopted vacua emerging in spontaneous symmetry breaking in quantum field theory (QFT) to describe memory. It was further developed by Stuart et al. at the end of the 1970s [12,23], where non-local memory storage and recall processes in the Takahashi model are described. Memory is vacua maintained by stability due to long-range correlation of massless Nambu–Goldstone (NG) bosons emerging in spontaneous symmetry breaking. The finite number of excitations of NG bosons represents memory recalling in the approach. In 1968, Fröhlich indicated that the physical coherence with long-range correlation might emerge in biological systems involving the boson condensation, where physical systems behave as a single entity, called the Fröhlich condensate [24,25]. In 1976, Davydov and Kislukha suggested a physical model for solitary waves propagating along protein α-helical structures, called the Davydov soliton [26]. The Fröhlich condensate and the Davydov soliton appear as static and dynamical properties in the nonlinear Schrödinger equation involving an equivalent Hamiltonian [27]. In the 1980s, Del Giudice et al. studied quantum theory for biological systems [28–31]. Especially, the QFT for water-rotational fields and photon fields describe laser-like phenomena in water–photon systems [30]. In the 1990s, Jibu and Yasue provided concrete degrees of freedom in QBD, namely water electric dipole fields and photon fields. [32,33] In 1994, Jibu et al. suggested super-radiance phenomena induced by microtubules (spontaneous cooperative coherent photon emission) [34], which might induce holographic memory storage suggested by Pribram [14,35,36]. In 1997, Jibu suggested quantum tunneling of photons among coherent domains represented by Josephson phenomena to achieve information transfer in a brain [37]. In 1995, Vitiello proposed squeezed coherent states involving NG bosons in a dissipative model of QBD regarding a brain as an open system [8]. The heterogeneity of memories can be represented by diverse unitarily inequivalent squeezed coherent states emerging due to infinite degrees of freedom in QFT.

Experimentally, Zheng and Pollack discovered the Exclusion Zone (EZ) water around hydrophilic surfaces, which excludes solutes [38]. Del Giudice et al. suggested that the properties of EZ water resemble those in coherent water suggested in QFT [39]. Furthermore, it is experimentally suggested that the Near-Infrared spectra of liquid water indicate the existence of a coherent water state [40]. The fractality of water systems is then found to emerge as scale-free phenomena significant in the auto-organization of complex systems,

such as ecosystems, neuron net and cellular metabolism. In a cortical system, neuronal avalanches indicate power-law behaviors and emerge as a scale-free phenomenon [41]. Moreover, magnetoencephalographic data suggest that fractal-like brain functional networks emerge [42]. Thus the analysis of fractal-like phenomena in a brain has been a prospective approach.

Fractals are isomorphic to squeezed coherent states, as suggested by Vitiello [43,44]. Self-similarity patterns in fractals represent scale-free phenomena in physical systems. Scale-free properties emerge as fixed points in the Renormalization Group (RG). The RG method was argued by Stüeckelberg and Petermann [45] and by Gell-Mann and Low [46] and applied to statistical physics by Wilson and Kogut [47]. In calculating quantum corrections in QFT, we encounter ultra-violet (UV) divergences. The divergences are renormalized by a finite number of counter-terms in each QFT model if the model is a renormalizable theory. In renormalization, we then encounter the arbitrariness of finite parts in counter-terms in renormalization prescription. To achieve the invariance of theory under renormalization prescription, physical parameters such as mass and coupling can evolve in changing physical scales as coarse graining procedures, which are described by RG equations [47–49]. In RG, the contributions in smaller scales are renormalized into parameters such as mass and coupling as coarse graining procedures, and we then encounter an effective theory in macroscopic scales (from microscopic scales) adopted to describe multi-scale brain functions in the beginning with the QBD Lagrangian and provide diversity in the effective theory for multi-scales in QBD. To derive RG equations for parameters, we need to analyze ultra-violet (UV) divergences appearing in self-energy and vertex corrections for cancellation of divergences by counter-terms in each QFT model. We might encounter fixed points where physical parameters become independent of renormalization scales for further coarse graining. The fixed points in RG represent scale-free fractal-like phenomena.

The aim of this paper is to cancel ultra-violet divergences in self-energy and vertex functions by counter-terms in the renormalization in QBD in $3 + 1$ dimensions. We begin with the Lagrangian density in QBD and expand terms involving counter-terms for renormalization. We next calculate self-energy and vertex functions and cancel ultra-violet divergences by counter-terms in renormalizations. We extend our analysis to the 2-Particle-Irreducible (2PI) effective action technique [50,51] in the derivation of Kadanoff–Baym (KB) equations [52–54]. Counter-terms will be adopted to achieve the cancellation of UV divergences in lattice simulations for the time-evolution of KB equations in QBD. Properties of divergences will be used in deriving RG equations in future studies, where fixed point solutions might describe the fractality of water–photon systems. Recently, we have shown a super-radiant solution in water–photon systems in $3 + 1$ dimensions, cooperative spontaneous photon emission [13]. Next, we have proposed the integration of QBD and holography using super-radiance and investigated the time-evolution of holograms [14]. Furthermore, we have provided control theory of coherent fields in the ϕ^4 model toward manipulating holograms or our subjective experiences [15]. The present work provides renormalization of UV divergences in quantum corrections in an interacting water–photon system, which will open up a new way to describe time-evolving holograms involving incoherent dipoles and photons, provide a control theory of holograms and introduce a RG method for QBD.

Our paper is organized as follows. In Section 2, we introduce the Lagrangian density for QBD with counter-terms. In Section 3, we calculate ultra-violet divergences in self-energy and vertex functions. In Section 4, we extend our approach to 2PI effective action technique. In Section 5, we discuss our results. In Section 6, we provide concluding remarks and perspectives. We adopt the natural unit with the light speed and the Planck constant divided by 2π set to unity. The metric tensor is set to be $g_{\mu\nu} = \text{diag}(1, -1, -1, -1)$ with space-time subscript $\mu, \nu = 0, 1, 2, 3$ and spatial subscript $i, j, n = 1, 2, 3$.

2. Lagrangian Density

In this section, we introduce the Lagrangian density for Quantum Brain Dynamics in $3 + 1$ dimensions and show Feynman diagrams for propagators of renormalized fields and counter terms for mass and vertices.

First, we begin with the Lagrangian density for QBD in $3 + 1$ dimensions based on [13,30]. It is written by,

$$
\begin{aligned}
\mathcal{L} &= -\frac{1}{4}F^{\mu\nu}[A(x)]F_{\mu\nu}[A(x)] - \frac{(\partial^i A_i)^2}{2\xi} + \int d\theta d\varphi \sin\theta\, \Psi^*(x,\theta,\varphi)\left[i\frac{i\partial}{\partial x^0} + \frac{\nabla_i^2}{2m} - \frac{\mathbf{l}^2}{2I}\right]\Psi(x,\theta,\varphi) \\
&\quad + \mu_c \int d\theta d\varphi \sin\theta\, \Psi^*(x,\theta,\varphi)\Psi(x,\theta,\varphi) \\
&\quad + 2ed_e\mathbf{E}\cdot\int d\theta d\varphi \sin\theta\, \Psi^*(x,\theta,\varphi)(\sin\theta\cos\varphi, \sin\theta\sin\varphi, \cos\theta)\Psi(x,\theta,\varphi),
\end{aligned}
\tag{1}
$$

with $F^{\mu\nu} = \partial^\mu A^\nu - \partial^\nu A^\mu$ with electric scalar potential A^0 and magnetic vector potential A^i ($i = 1, 2, 3$), electric field $E_i = -\partial_i A_0 + \partial_0 A_i$, dipole fields $\Psi^{(*)}(x,\theta,\varphi)$, the gauge fixing parameter $\xi = 1$, mass of dipoles m, moment of inertia for dipoles I with $\frac{1}{I} = 4\,\text{meV}$, chemical potential μ_c and dipole moment for a water molecule $2ed_e$ with elementary charge e and $d_e = 0.2\,\text{Å}$. We adopt the temporal axial gauge $A^0 = 0$. We assume the isotropic moment of inertia I for water dipoles. We adopt the two-energy-level approximation for angular momentum squared $\mathbf{l}^2 = -\left(\frac{1}{\sin^2\theta}\frac{\partial^2}{\partial\varphi^2} + \frac{1}{\sin\theta}\frac{\partial}{\partial\theta}\left(\sin\theta\frac{\partial}{\partial\theta}\right)\right)$ for rotational degrees of freedom of water dipoles. We expand water electric dipole fields by the dipole field for the ground state $\psi_s(x)$ and the dipole fields for the 1st excited states $\psi_\alpha(x)$ with $\alpha = 0, \pm 1$ as,

$$
\Psi(x,\theta,\varphi) = \psi_s(x)Y_{00}(\theta,\varphi) + \sum_{\alpha=0,\pm1}\psi_\alpha(x)Y_{1\alpha}(\theta,\varphi),
\tag{2}
$$

$$
\Psi^*(x,\theta,\varphi) = \psi_s^*(x)Y_{00}^*(\theta,\varphi) + \sum_{\alpha=0,\pm1}\psi_\alpha^*(x)Y_{1\alpha}^*(\theta,\varphi),
\tag{3}
$$

using the spherical harmonics for the ground state $Y_{00}(\theta,\varphi)$ corresponding to the eigenvalue $\mathbf{l}^2 = 0$ and the 1st excited states $Y_{1\alpha}(\theta,\varphi)$ with $\alpha = 0, \pm 1$ corresponding to eigenvalues $\mathbf{l}^2 = 2$ shown by,

$$
Y_{00}(\theta,\varphi) = \frac{1}{\sqrt{4\pi}},
\tag{4}
$$

$$
Y_{1\pm1}(\theta,\varphi) = \mp i\sqrt{\frac{3}{8\pi}}\sin\theta\, e^{\pm i\varphi}, \quad Y_{10}(\theta,\varphi) = i\sqrt{\frac{3}{4\pi}}\cos\theta.
\tag{5}
$$

The 1st and 2nd terms in Equation (1) are rewritten as,

$$
-\frac{1}{4}F^{\mu\nu}[A(x)]F_{\mu\nu}[A(x)] - \frac{(\partial^i A_i)^2}{2} = \frac{1}{2}(\partial^\mu A_i)(\partial_\mu A_i).
\tag{6}
$$

The 3rd term in Equation (1) is then written as,

$$
\begin{aligned}
\int d\theta d\varphi \sin\theta\, \Psi^*(x,\theta,\varphi)\left[i\frac{i\partial}{\partial x^0} + \frac{\nabla_i^2}{2m} - \frac{\mathbf{l}^2}{2I}\right]\Psi(x,\theta,\varphi) &= \psi_s^*\left(i\frac{\partial}{\partial x^0} + \frac{\nabla_i^2}{2m}\right)\psi_s \\
&\quad + \sum_{\alpha=0,\pm1}\psi_\alpha^*\left(i\frac{\partial}{\partial x^0} + \frac{\nabla_i^2}{2m} - \frac{1}{I}\right)\psi_\alpha
\end{aligned}
\tag{7}
$$

The 4th term in Equation (1) is written by,

$$\mu_c \int d\theta d\varphi \sin\theta \, \Psi^*(x,\theta,\varphi)\Psi(x,\theta,\varphi) = \mu_c\left(\psi_s^*\psi_s + \sum_\alpha \psi_\alpha^*\psi_\alpha\right). \tag{8}$$

The 5th term in Equation (1) with the electric fields $E_i = -F^{0i}$ ($i = 1,2,3$) by,

$$2ed_e \int_0^{2\pi} d\varphi \int_0^\pi d\theta \sin\theta \, \Psi^*(\sin\theta\cos\varphi, \sin\theta\sin\varphi, \cos\theta)_i \Psi E_i = \mathcal{M}_i(x)E_i(x), \tag{9}$$

with the dipole moment density $\mathcal{M}_i$ ($i = 1,2,3$) defined as,

$$\mathcal{M}_1 = \frac{2ed_e i}{\sqrt{6}}\left(\psi_s^*\psi_{-1} - \psi_s^*\psi_1 + \psi_1^*\psi_s - \psi_{-1}^*\psi_s\right), \tag{10}$$

$$\mathcal{M}_2 = \frac{2ed_e}{\sqrt{6}}\left(\psi_s^*\psi_{-1} + \psi_s^*\psi_1 + \psi_1^*\psi_s + \psi_{-1}^*\psi_s\right), \tag{11}$$

$$\mathcal{M}_3 = \frac{2ed_e i}{\sqrt{3}}\left(\psi_s^*\psi_0 - \psi_0^*\psi_s\right). \tag{12}$$

We can then rewrite as,

$$\begin{aligned}
\mathcal{M}_i(x)E_i(x) &= \frac{2ed_e}{\sqrt{6}}\Bigg[(iE_1 + E_2)(\psi_s^*\psi_{-1} + \psi_1^*\psi_s) + (-iE_1 + E_2)(\psi_s^*\psi_1 + \psi_{-1}^*\psi_s) \\
&\quad + \sqrt{2}iE_3(\psi_s^*\psi_0 - \psi_0^*\psi_s)\Bigg] \\
&= \frac{2ed_e}{\sqrt{6}} \sum_{\alpha=0,\pm1}\Bigg[\left(-i\alpha(E_1 + i\alpha E_2) + \sqrt{2}i(1 - |\alpha|)E_3\right)\psi_s^*\psi_\alpha \\
&\quad + \left(i\alpha(E_1 - i\alpha E_2) - \sqrt{2}i(1 - |\alpha|)E_3\right)\psi_\alpha^*\psi_s\Bigg].
\end{aligned} \tag{13}$$

Next, we rewrite the Lagrangian density with several counter terms. Using the bare fields $A_{b,i} = Z_{ph}^{\frac{1}{2}}A_i$ with $i = 1,2,3$ (with $E_{b,i} = Z_{ph}^{\frac{1}{2}}E_i$), $\psi_{b,s}^{(*)} = Z_s^{\frac{1}{2}}\psi_s^{(*)}$, and $\psi_{b,\alpha}^{(*)} = Z_1^{\frac{1}{2}}\psi_\alpha^{(*)}$ ($\alpha = 0, \pm1$) involving the renormalization coefficient Z_{ph} with respect to wave functions for photons, coefficient Z_s for dipoles in the ground state and coefficient Z_1 for dipoles in the 1st excited state, we write the Lagrangian density in QBD by the bare fields as,

$$\begin{aligned}
\mathcal{L} &= -\frac{1}{4}F^{\mu\nu}[A_b]F_{\mu\nu}[A_b] - \frac{(\partial^i A_{b,i})^2}{2} \\
&\quad + \psi_{b,s}^*\left(i\frac{\partial}{\partial x^0} + \frac{\nabla_i^2}{2m_s}\right)\psi_{b,s} + \sum_{\alpha=0,\pm1}\psi_{b,\alpha}^*\left(i\frac{\partial}{\partial x^0} + \frac{\nabla_i^2}{2m_1} - \frac{1}{I_0}\right)\psi_{b,\alpha} \\
&\quad + \mu_0\left(\psi_{b,s}^*\psi_{b,s} + \sum_\alpha \psi_{b,\alpha}^*\psi_{b,\alpha}\right) \\
&\quad + \frac{2(ed_e)_0}{\sqrt{6}}\sum_\alpha\Bigg[\left(-i\alpha(E_{b,1} + i\alpha E_{b,2}) + \sqrt{2}i(1 - |\alpha|)E_{b,3}\right)\psi_{b,s}^*\psi_{b,\alpha} \\
&\quad \left(i\alpha(E_{b,1} - i\alpha E_{b,2}) - \sqrt{2}i(1 - |\alpha|)E_{b,3}\right)\psi_{b,\alpha}^*\psi_{b,s}\Bigg],
\end{aligned} \tag{14}$$

where we adopt the bare mass m_s and m_1, the bare moment of inertia I_0, the bare chemical potential μ_0 and the bare dipole moment $2(ed_e)_0$. The above Lagrangian density is rewritten as,

$$
\begin{aligned}
\mathcal{L} = {} & -\frac{1}{4} Z_{ph} F^{\mu\nu}[A] F_{\mu\nu}[A] - Z_{ph} \frac{(\partial^i A_i)^2}{2} \\
& + Z_s \psi_s^* \left(i\frac{\partial}{\partial x^0} + \frac{\nabla_i^2}{2m_s} \right) \psi_s + Z_1 \sum_{\alpha=0,\pm1} \psi_\alpha^* \left(i\frac{\partial}{\partial x^0} + \frac{\nabla_i^2}{2m_1} - \frac{1}{I_0} \right) \psi_\alpha \\
& + \mu_0 \left(Z_s \psi_s^* \psi_s + Z_1 \sum_\alpha \psi_\alpha^* \psi_\alpha \right) \\
& + \frac{2(ed_e)_0}{\sqrt{6}} Z_{ph}^{\frac{1}{2}} Z_s^{\frac{1}{2}} Z_1^{\frac{1}{2}} \sum_\alpha \left[\left(-i\alpha(E_1 + i\alpha E_2) + \sqrt{2}i(1-|\alpha|)E_3 \right) \psi_s^* \psi_\alpha \right. \\
& \left. \left(i\alpha(E_1 - i\alpha E_2) - \sqrt{2}i(1-|\alpha|)E_3 \right) \psi_\alpha^* \psi_s \right].
\end{aligned} \tag{15}
$$

Next, we introduce the parameters as follows,

$$
\delta_{Z_{ph}} = Z_{ph} - 1, \qquad \delta_{Z_s} = Z_s - 1, \qquad \delta_{Z_1} = Z_1 - 1,
$$

$$
\delta_{m_s^{-1}} = \frac{Z_s}{m_s} - \frac{1}{m}, \qquad \delta_{m_1^{-1}} = \frac{Z_1}{m_1} - \frac{1}{m}, \qquad \delta_{I^{-1}} = \frac{Z_1}{I_0} - \frac{1}{I},
$$

$$
\delta_{\mu,s} = Z_s \mu_0 - \mu_c, \quad \delta_{\mu,1st} = Z_1 \mu_0 - \mu_c, \quad \delta_{ed_e} = (ed_e)_0 Z_{ph}^{\frac{1}{2}} Z_s^{\frac{1}{2}} Z_1^{\frac{1}{2}} - ed_e. \tag{16}
$$

Then the Lagrangian density is rewritten as,

$$
\begin{aligned}
\mathcal{L} = {} & \frac{1}{2} (\partial^\nu A_i)(\partial_\nu A_i) + \psi_s^* \left(i\frac{\partial}{\partial x^0} + \frac{\nabla_i^2}{2m} + \mu_c \right) \psi_s + \sum_{\alpha=0,\pm1} \psi_\alpha^* \left(i\frac{\partial}{\partial x^0} + \frac{\nabla_i^2}{2m} - \frac{1}{I} + \mu_c \right) \psi_\alpha \\
& + \frac{2ed_e}{\sqrt{6}} \sum_{\alpha=0,\pm1} \left[\left(-i\alpha(E_1 + i\alpha E_2) + \sqrt{2}i(1-|\alpha|)E_3 \right) \psi_s^* \psi_\alpha \right. \\
& \left. + \left(i\alpha(E_1 - i\alpha E_2) - \sqrt{2}i(1-|\alpha|)E_3 \right) \psi_\alpha^* \psi_s \right] \\
& + \frac{1}{2} \delta_{Z_{ph}} (\partial^\nu A_i)(\partial_\nu A_i) + \psi_s^* \left(\delta_{Z_s} i\frac{\partial}{\partial x^0} + \frac{\delta_{m_s^{-1}} \nabla_i^2}{2} + \delta_{\mu,s} \right) \psi_s \\
& + \sum_\alpha \psi_\alpha^* \left(\delta_{Z_1} i\frac{\partial}{\partial x^0} + \frac{\delta_{m_1^{-1}} \nabla_i^2}{2} - \delta_{I^{-1}} + \delta_{\mu,1st} \right) \psi_\alpha \\
& + \frac{2\delta_{ed_e}}{\sqrt{6}} \sum_{\alpha=0,\pm1} \left[\left(-i\alpha(E_1 + i\alpha E_2) + \sqrt{2}i(1-|\alpha|)E_3 \right) \psi_s^* \psi_\alpha \right. \\
& \left. + \left(i\alpha(E_1 - i\alpha E_2) - \sqrt{2}i(1-|\alpha|)E_3 \right) \psi_\alpha^* \psi_s \right]. \tag{17}
\end{aligned}
$$

The 5th, 6th, 7th and 8th terms in the above Lagrangian represent counter-terms.

Finally, we show Feynman diagrams for propagators, vertices and counter-terms in Fourier transformation. Using the above Lagrangian density, we show the diagrams in Figure 1. The propagator for photons $D_{ij}(k)$, the propagator for dipoles in the ground state

$G_{ss}(p)$ and the propagators for dipoles in the 1st excited states $G_{\alpha\alpha}(p)$ with $\alpha = 0, \pm 1$ are written by,

$$D_{ij}(k) = \frac{i\delta_{ij}}{k^2 + i\epsilon}, \tag{18}$$

$$G_{ss}(p) = \frac{i}{p^0 - \frac{\mathbf{p}^2}{2m} + \mu_c + i\epsilon}, \tag{19}$$

$$G_{\alpha\alpha}(p) = \frac{i}{p^0 - \frac{\mathbf{p}^2}{2m} - \frac{1}{I} + \mu_c + i\epsilon}, \tag{20}$$

respectively. The vertices represent,

$$\frac{\delta^3 \int_z (i\mathcal{M}_i(z)E_i(z))}{\delta\psi_s(u_1)\delta\psi_\alpha^*(u_2)\delta A^j(u_3)} = \frac{2ed_e}{\sqrt{6}} \int_z \left[\alpha(\delta_j^1 - i\alpha\delta_j^2) - \sqrt{2}(1 - |\alpha|)\delta_j^3 \right]$$
$$\times \left(\partial_z^0 \delta(z - u_3) \right) \delta(z - u_1)\delta(z - u_2), \tag{21}$$

with matrix element $\langle \alpha | \cdot | k, s \rangle$ of $\int_z (i\mathcal{M}_i(z)E_i(z))$ (shown in Equation (13)) describing processes of incoming photons with factor $e^{-ik\cdot u_3}$, incoming dipoles in the ground state s with factor $e^{-ip\cdot u_1}$ and outgoing dipoles in 1st excited states α with factor $e^{il\cdot u_2}$ involving integration $\int_{u_1, u_2, u_3}$, and

$$\frac{\delta^3 \int_z (i\mathcal{M}_i(z)E_i(z))}{\delta\psi_s^*(w_1)\delta\psi_\alpha(w_2)\delta A^j(w_3)} = \frac{2ed_e}{\sqrt{6}} \int_z \left[-\alpha(\delta_j^1 + i\alpha\delta_j^2) + \sqrt{2}(1 - |\alpha|)\delta_j^3 \right]$$
$$\times \left(\partial_z^0 \delta(z - w_3) \right) \delta(z - w_1)\delta(z - w_2), \tag{22}$$

with $\langle k, s | \cdot | \alpha \rangle$ representing processes of outgoing photons with factor $e^{ik\cdot w_3}$, outgoing dipoles in the ground state with factor $e^{ip\cdot w_1}$ and incoming dipoles in the 1st excited states with factor $e^{-il\cdot w_2}$ involving integration $\int_{w_1, w_2, w_3}$. We show vertices in Figure 1. Here we find that the vertex with incoming dipoles in 1st excited states involves the factor with $(ik^0) \times \cdots$ and that the vertex with outgoing dipoles in 1st excited states involves the factor with $(-ik^0) \times \cdots$. Using Figure 1, we perform renormalization of self-energy and vertices in the next section.
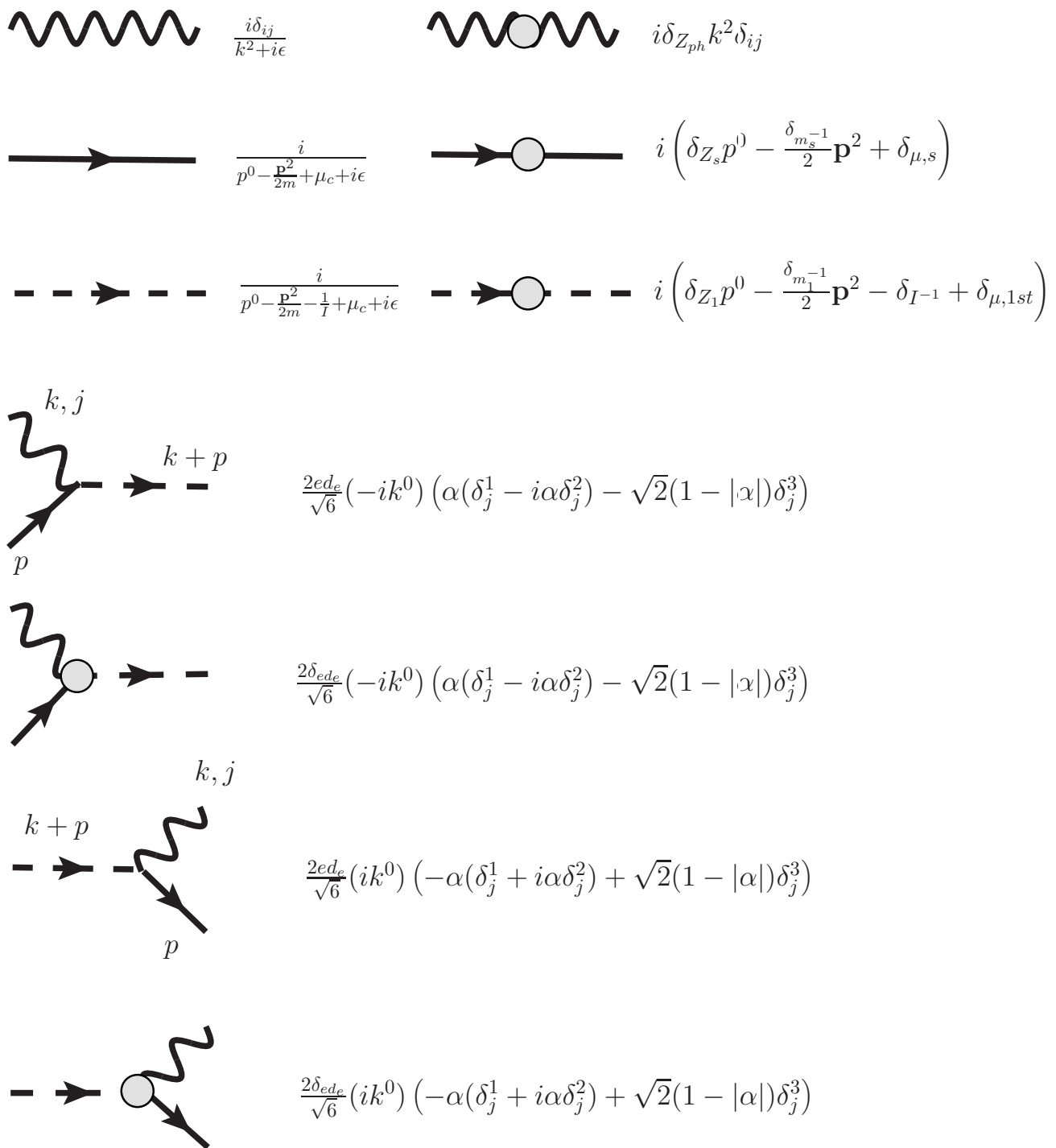
Figure 1. Diagrams for propagators, vertices and counter-terms. The wavy line represents a photon propagator with subscripts $i, j = 1, 2, 3$ for the polarization of photons, the solid line represents a dipole propagator for the ground state, and the dotted line represents a dipole propagator for the 1st excited states $\alpha = 0, \pm 1$. The gray-circle represents the counter-terms.

3. Renormalization

In this section, we write Feynman diagrams for self-energy and vertices and cancel ultra-violet (UV) divergences by counter-terms. We have referred to [49] for calculations.

3.1. 1-Loop Self-Energy

In this section, we show a 1-loop self-energy for photons and dipoles, and we find that UV divergences are canceled by counter-terms.

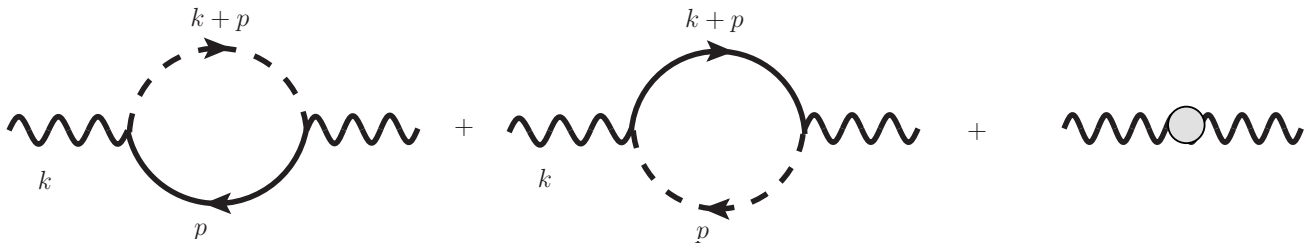First, we shall see the self-energy for photons $\Pi_{ij}(k)$ in 1-loop order shown in Figure 2.

Figure 2. Self-energy for photons in 1-loop order and counter-term.

We find that 1-loop self-energy for photons contains the factor,

$$
\begin{aligned}
\int_p G_{\alpha\alpha}(k+p)G_{ss}(p) &\sim \int \frac{dp^0}{2\pi} \frac{i}{p^0 - \frac{\mathbf{p}^2}{2m} + \mu_c + i\epsilon} \cdot \frac{i}{p^0 - \frac{\mathbf{p}^2}{2m} - \frac{1}{I} + \mu_c + i\epsilon} \\
&= \int_0^1 dx \int \frac{dp^0}{2\pi} \frac{-1}{\left[p^0 + xk^0 - \frac{(1-x)\mathbf{p}^2}{2m} - \frac{x(\mathbf{p}+\mathbf{k})^2}{2m} - \frac{x}{I} + \mu_c + i\epsilon\right]^2} \\
&= 0,
\end{aligned}
\tag{23}
$$

with $\int_p = \int \frac{d^4 p}{(2\pi)^4}$, since the 1st derivative of residue -1 by p^0 is zero. Here we have used the Feynman's formula,

$$
\frac{1}{AB} = \int_0^1 dx \frac{1}{[xA + (1-x)B]^2}.
\tag{24}
$$

Similarly, we also find the relation,

$$
\int_p G_{ss}(k+p)G_{\alpha\alpha}(p) = 0.
\tag{25}
$$

As a result, the self-energy for photons in 1-loop order is zero. We then find $\delta_{Z_{ph}} = 0$ or $Z_{ph} = 1$ in 1-loop order.

Next, we shall see self-energy for dipoles in 1st excited states, as shown in Figure 3. Using the Feynman rules in Figure 1, the self-energy $\Sigma_{\alpha\alpha}$ with $\alpha = 0, \pm 1$ can be written by,

$$
\Sigma_{\alpha\alpha}(p) = -\frac{4}{3}(ed_e)^2 \int_k (k^0)^2 \frac{i}{p^0 - k^0 - \frac{(\mathbf{p}-\mathbf{k})^2}{2m} + \mu_c + i\epsilon} \cdot \frac{i}{k^2 + i\epsilon}.
\tag{26}
$$

The detailed calculations are shown in Appendix A. The result is given by,

$$
\Sigma_{\alpha\alpha}(p) = -\frac{4i}{3}(ed_e)^2 \int_0^1 dx \int_{l_E} \frac{[\text{numerator 1}]}{(l_E^2 + x^2 m^2)^2},
\tag{27}
$$

where the subscript E represents the Euclidean 4-dimensional momenta, and [numerator 1] represents,

$$[\text{numerator 1}] = (l_E^0)^2\left[|\mathbf{l}_E| + (1-3x)\left(m+p^0+\mu_c\right) + \frac{(1-x)^2\mathbf{p}^2+m^2}{2|\mathbf{l}_E|} - \frac{(1-x)^2\mathbf{p}^2}{6|\mathbf{l}_E|}\right]$$
$$-x^2|\mathbf{l}_E|m\left(m+2\left(p^0+\mu_c\right)\right) - x^2(1-x)m^2\left(m+3\left(p^0+\mu_c\right)\right)$$
$$+\frac{4mx(1-x)}{l_E^2+x^2m^2}\left((1-3x)(l_E^0)^2m+(l_E^0)^2|\mathbf{l}_E|\right)\left(p^0+\mu_c-\frac{\mathbf{p}^2}{2m}\right). \tag{28}$$

We find $\Sigma_{\alpha\alpha}(p)$ involves cubic, quadratic, linear and logarithmic divergences in Equation (27); for example, the term $(l_E^0)^2|\mathbf{l}_E|$ in [numerator 1] in Equation (28) induces cubic divergence. They are canceled by counter-terms in Figures 1 and 3. We then find the relation,

$$\delta_{Z_1}p^0 - \frac{\delta_{m_1^{-1}}\mathbf{p}^2}{2} - \delta_{I^{-1}} + \delta_{\mu,1st} = \frac{4}{3}(ed_e)^2\int_0^1 dx\int_{l_E}\frac{[\text{numerator 1}]}{(l_E^2+x^2m^2)^2}. \tag{29}$$

We find that δ_{Z_1} and $\delta_{m_1^{-1}}$ are independent of the chemical potential μ_c.
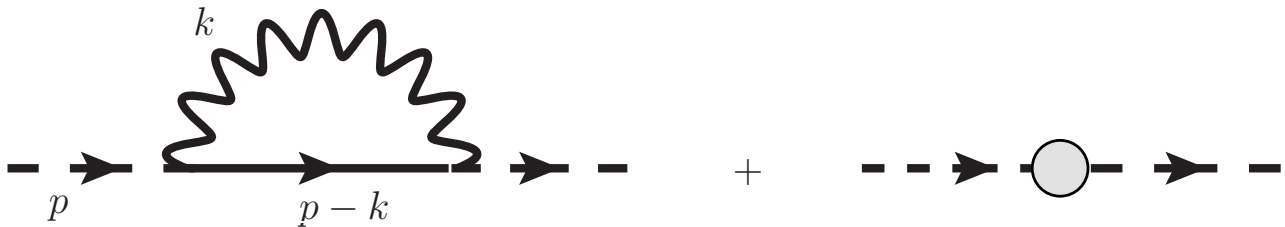

Figure 3. Self-energy for dipoles in 1st excited states in 1-loop order and counter-term.

Finally, we show counter-terms for Σ_{ss}. Since we can write,

$$\Sigma_{ss}(p) = -\frac{4}{3}(ed_e)^2\sum_{\alpha=0,\pm1}\int_k(k^0)^2\frac{i}{p^0-k^0-\frac{(\mathbf{p}-\mathbf{k})^2}{2m}-\frac{1}{I}+\mu_c+i\epsilon}\cdot\frac{i}{k^2+i\epsilon}$$
$$= -4(ed_e)^2\int_k(k^0)^2\frac{i}{p^0-k^0-\frac{(\mathbf{p}-\mathbf{k})^2}{2m}-\frac{1}{I}+\mu_c+i\epsilon}\cdot\frac{i}{k^2+i\epsilon}, \tag{30}$$

the counter-terms can be derived by changing coefficient $\frac{4}{3}$ to 4 and factor μ_c to $\mu_c-\frac{1}{I}$ for $\Sigma_{\alpha\alpha}(p)$ in Equation (26). We can then derive,

$$\delta_{Z_s}p^0 - \frac{\delta_{m_s^{-1}}\mathbf{p}^2}{2} + \delta_{\mu,s} = 4(ed_e)^2\int_0^1 dx\int_{l_E}\frac{[\text{numerator 2}]}{(l_E^2+x^2m^2)^2}, \tag{31}$$

with,

$$[\text{numerator 2}] = (l_E^0)^2\left[|\mathbf{l}_E| + (1-3x)\left(m+p^0+\mu_c-\frac{1}{I}\right) + \frac{(1-x)^2\mathbf{p}^2+m^2}{2|\mathbf{l}_E|} - \frac{(1-x)^2\mathbf{p}^2}{6|\mathbf{l}_E|}\right]$$
$$-x^2|\mathbf{l}_E|m\left(m+2\left(p^0+\mu_c-\frac{1}{I}\right)\right) - x^2(1-x)m^2\left(m+3\left(p^0+\mu_c-\frac{1}{I}\right)\right)$$
$$+\frac{4mx(1-x)}{l_E^2+x^2m^2}\left((1-3x)(l_E^0)^2m+(l_E^0)^2|\mathbf{l}_E|\right)\left(p^0+\mu_c-\frac{1}{I}-\frac{\mathbf{p}^2}{2m}\right). \tag{32}$$

3.2. 1-Loop 3-Point Vertex

In this section, we show a 1-loop 3-point vertex and find that UV divergences are canceled by a counter-term. We shall see a 1-loop 3-point vertex shown in Figure 4.
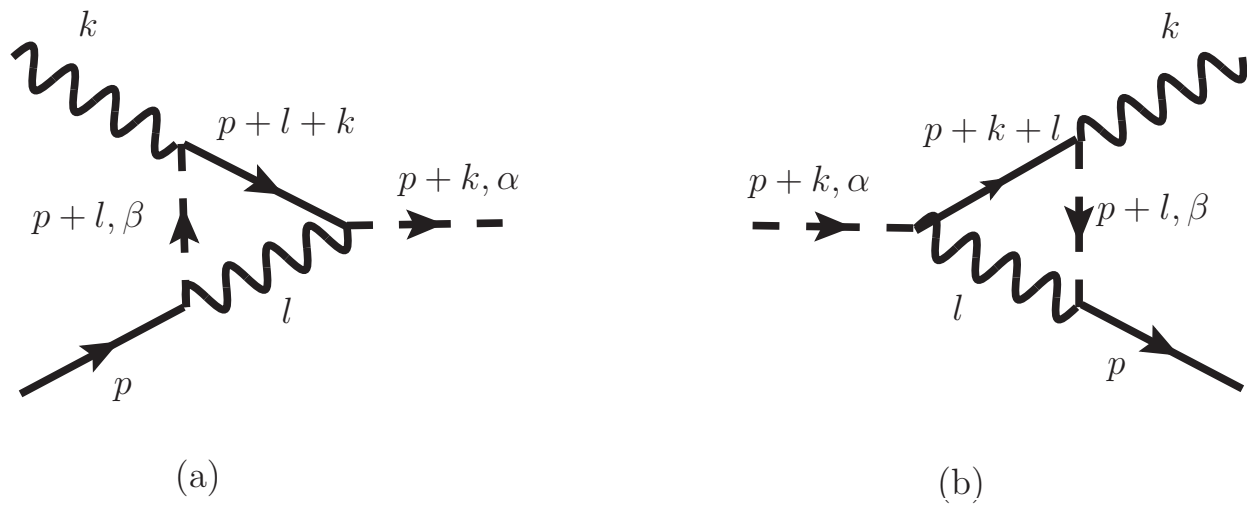
Figure 4. 1-loop 3-point vertices. (**a**) Dipoles in the ground state absorb photons and dipoles in 1st excited states are emitted. (**b**) Inverse processes of (**a**).

The UV divergences in this figure are canceled by counter-terms involving δ_{ed_e} for vertices in Figure 1. The diagram in Figure 4a represents the term given by,

$$
\begin{aligned}
\text{vertex (a)} \;=\; & \int_l \sum_\beta \left(\frac{2ed_e}{\sqrt{6}}\right)^3 (-il^0)\left[\beta\left(\delta_j^1 - i\beta\delta_j^2\right) - \sqrt{2}(1-|\beta|)\delta_j^3\right] \\
& \times (-il^0)\left[\alpha\left(\delta_n^1 - i\alpha\delta_n^2\right) - \sqrt{2}(1-|\alpha|)\delta_n^3\right]\delta^{jn} \\
& \times (ik^0)\left[-\beta\left(\delta_i^1 + i\beta\delta_i^2\right) + \sqrt{2}(1-|\beta|)\delta_i^3\right] \\
& \times \frac{i}{l^2+i\epsilon} \times \frac{i}{p^0+l^0-\frac{(\mathbf{p+l})^2}{2m}-\frac{1}{I}+\mu_c+i\epsilon} \times \frac{i}{p^0+l^0+k^0-\frac{(\mathbf{p+l+k})^2}{2m}+\mu_c+i\epsilon}.
\end{aligned}
\tag{33}
$$

The detailed calculations are given in Appendix B. We encounter the counter-term δ_{ed_e} as,

$$
\begin{aligned}
-\frac{2\delta_{ed_e}}{\sqrt{6}} \;=\; & -4\left(\frac{2ed_e}{\sqrt{6}}\right)^3 \int_0^1 dx \int_0^1 dy \int_{q_E} \frac{-1}{(q_E^2+(x+y)^2m^2)^3} \\
& \times \Bigg[(q_E^0)^2\Bigg[(q_E^0)^2 - \Bigg(|\mathbf{q}_E|^2 + 6m^2(x+y)(x+y-1) + 2m|\mathbf{q}|(1-3(x+y)) + 2m^2 \\
& + \frac{1}{I^2}\left(5(y-x)^2 + \frac{3y^2-3y+1}{3} - \left((1-x)^2 - y^2\right) - 2y(1-x-y)mI\right)\Bigg)\Bigg] \\
& + |\mathbf{q}_E^2|\left[(x+y)^2m^2 + \frac{(y-x)^2}{I^2}\right] \\
& - (q_E^0)^2\left((q_E^0)^2 - |\mathbf{q}_E|^2\right)\frac{\frac{3}{I^2}(x^2-x-2xy)}{q_E^2+(x+y)^2m^2}\Bigg].
\end{aligned}
\tag{34}
$$

The vertex correction involves quadratic, linear and logarithmic divergences canceled by counter-terms with δ_{ed_e}. We have derived the counter-term for 1-loop vertex correction. We can derive the same result from Figure 4b.

3.3. 2-Loop Self-Energy

In this section, we estimate divergences in self-energy in 2-loop order.

First, we shall investigate the self-energy 1 for photons in Figure 5. This diagram contains the following factor,

$$\int_l (l^0)^2 \int_p G_{ss}(p) G_{\alpha\alpha}(p - l) G_{ss}(p - l - k) G_{\beta\beta}(p - k)$$

$$\sim (l^0)^2 \int_0^1 dx \int_0^1 dy \int_0^1 dz \int_0^1 dw \delta(x + y + z + w - 1) \int_{p^0} \frac{1}{(p^0 + f(x, y, z, w, \mathbf{p}, k, l))^4}, \quad (35)$$

where we have used the Feynman's formula. The function f is independent of p^0. Since the 3rd derivative of residue one by p^0 is zero, the contribution of this diagram is zero.
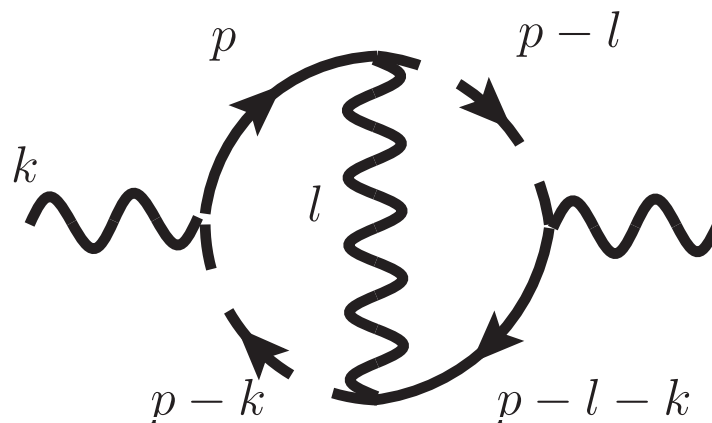

Figure 5. Self-energy 1 for photons in 2-loop order.

Next, we shall estimate the self-energy 2 on the left of Figure 6. This diagram contains a divergent part of the propagator of dipoles in the ground state, which can be canceled by the right diagram with counter-term. Even if the finite part, such as Cp^0 with finite constant C remains after the cancellation, by using Feynman's formula,

$$\frac{1}{AB^2} = \int_0^1 dx \int_0^1 dy \delta(x + y - 1) \frac{2y}{(xA + yB)^3}, \quad (36)$$

we encounter the form of

$$\int_p \frac{i}{p^0 - k^0 - \frac{(\mathbf{p} - \mathbf{k})^2}{2m} - \frac{1}{l} + \mu_c + i\epsilon} \cdot \frac{i}{p^0 - \frac{\mathbf{p}^2}{2m} + \mu_c + \epsilon} \cdot \frac{iCp^0}{p^0 - \frac{\mathbf{p}^2}{2m} + \mu_c + \epsilon} \sim \int_{p^0} \frac{Cp^0}{(p^0 + g(x, y, \mathbf{p}, k))^3}, \quad (37)$$

where g is a function independent of p^0. Since the 2nd derivative of the residue Cp^0 by p^0 is zero, the remaining part in the above equation is zero. The same estimation is possible for the case when the propagator of dipoles in the 1st excited states contains divergent self-energy in the inner loop. We find $\delta_{Z_{ph}}$ is zero or $Z_{ph} = 1$ in 2-loop order.
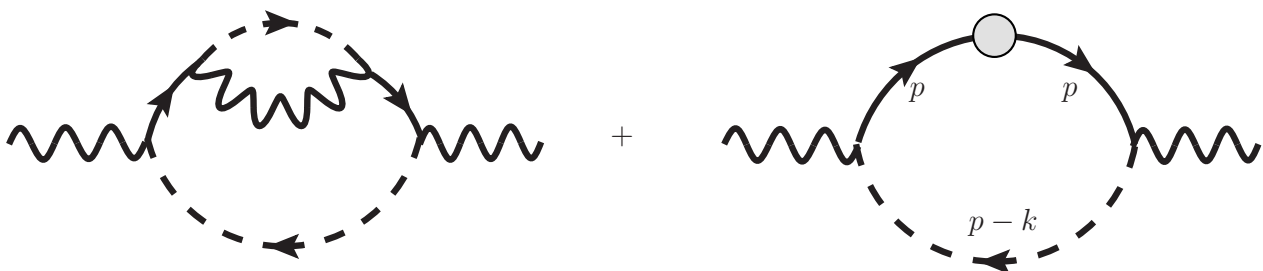

Figure 6. Self-energy 2 for photons in 2-loop order and self-energy with counter-term.

Next, we shall estimate the self-energy for dipoles in the ground state in 2-loop order in the left diagram in Figure 7a. This diagram contains quadratic divergences from vertex correction times cubic divergences from the remaining part. The quadratic divergences from vertex corrections are canceled by the two middle diagrams in Figure 7a with counter-terms. The sum of the left diagram and these middle diagrams contains cubic divergence in their loops. The cubic divergence can be canceled by the right counter-term in a similar way to 1-loop self-energy. We estimate the self-energy in the left diagram in Figure 7b. This diagram involves cubic divergence in the inner loop. The cubic divergence is canceled by the middle diagram with a counter-term. The sum of the left and middle diagrams contains cubic divergence at most. The cubic divergence can be canceled by the right counter-term in a similar way to 1-loop self-energy. We can also estimate the self-energy in Figure 7c. This diagram contains zero contributions in inner loops so the contribution is zero.
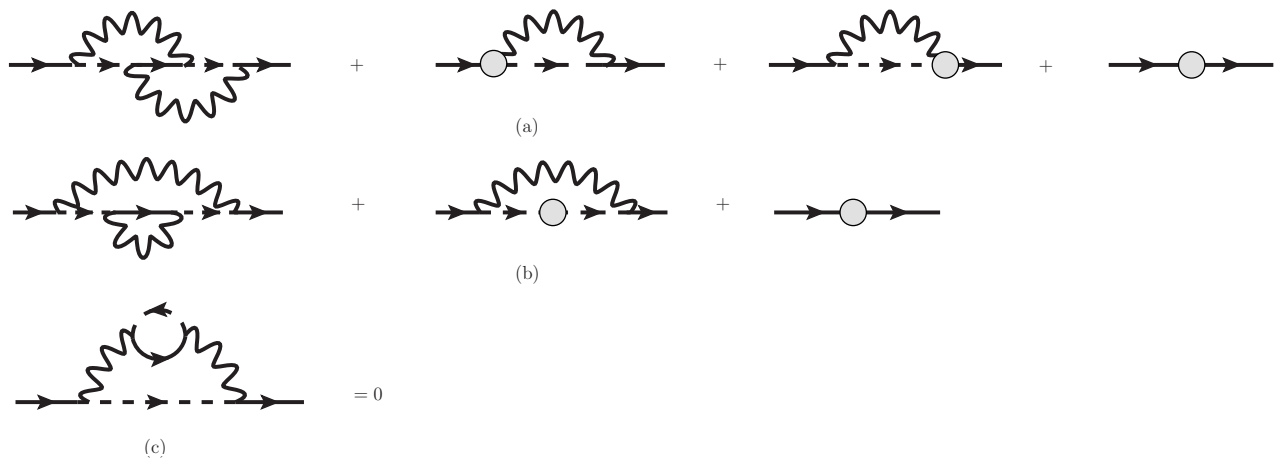

Figure 7. Self-energy for dipoles in the ground state in 2-loop order and counter-terms.

Finally, we shall show the self-energy for dipoles in the 1st excited states in Figure 8. The estimation of divergences is similar to the cases of self-energy for dipoles in the ground state. We just need to show the labels of external lines for dipoles in the 1st excited states α and β will be the same one. The labels $\alpha, \beta = 0, \pm 1$ represent the three 1st excited states in our model originating from spherical harmonics $Y_{1\alpha}$ for rotational degrees of freedom of dipoles. We can consider the three cases shown in Figure 8d, where there are two incoming dipoles in 1st excited states to vertices connected by photon propagator (left), two outgoing dipoles in 1st excited states to vertices connected by propagator (middle), and one incoming and one outgoing dipole in 1st excited states connected by propagator (right). In the right diagram, we encounter the factor,

$$\delta^{ij}\left[\alpha(\delta_i^1 - i\alpha\delta_i^2) - \sqrt{2}(1 - |\alpha|)\delta_i^3\right]\left[-\beta(\delta_j^1 + i\beta\delta_j^2) + \sqrt{2}(1 - |\beta|)\delta_j^3\right]$$
$$= -\alpha\beta - \alpha^2\beta^2 - 2(1 - |\alpha|)(1 - |\beta|), \tag{38}$$

where we have used the Feynman rules in Figure 1. In $\alpha = 1$, this factor is nonzero only when $\beta = 1$. (In $\alpha = 0$, it is nonzero only when $\beta = 0$). We find that this factor is nonzero only in the cases $\alpha = \beta$ in the right diagram in Figure 8d. We shall consider the middle diagram. It contains the factor

$$\delta^{ij}\left[\alpha(\delta_i^1 - i\alpha\delta_i^2) - \sqrt{2}(1 - |\alpha|)\delta_i^3\right]\left[\beta(\delta_j^1 - i\beta\delta_j^2) - \sqrt{2}(1 - |\beta|)\delta_j^3\right]$$
$$= \alpha\beta - \alpha^2\beta^2 + 2(1 - |\alpha|)(1 - |\beta|). \tag{39}$$

This factor is nonzero only in $\alpha = -\beta$. Similarly, we find that the left diagram is nonzero only in $\alpha = -\beta$. Using these rules, we find that nonzero contributions are only in $\alpha = -\gamma$ and $\gamma = -\beta$ in the left diagram in Figure 8a, so we find $\alpha = \beta$. In the left diagram

in Figure 8b, we also find $\alpha = \beta$. In self-energy for dipoles in 1st excited states, the label of incoming dipoles α is equal to that of outgoing dipoles β at least in 1-loop and 2-loop order.
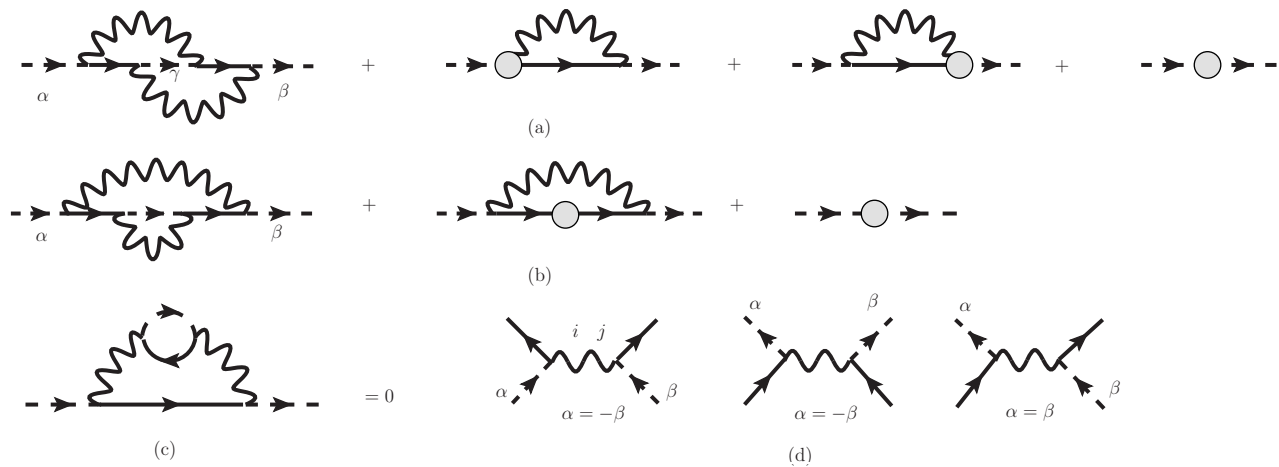

Figure 8. Self-energy for dipoles in the 1st excited states in 2-loop order and counter-terms.

4. Renormalization in 2-Particle-Irreducible Effective Action Technique

In this section, we write 2-Particle-Irreducible (2PI) effective action [50,51,55] with counter-terms in Quantum Brain Dynamics and describe how to cancel ultra-violet diagrams in self-energy by counter-terms in the Kadanoff–Baym equations.

Beginning with the Lagrangian density in QBD in Equation (17), we can derive 2PI effective action. The action Γ_{2PI} is given by,

$$
\begin{aligned}
\Gamma_{2PI} \quad = \quad & \frac{i}{2}\ln D^{-1} + \frac{i}{2}\mathrm{Tr}D_0^{-1}D + i\ln G_{ss}^{-1} + i\mathrm{Tr}G_{0,ss}^{-1}G_{ss} \\
& + \sum_{\alpha}\Big[i\ln G_{\alpha\alpha}^{-1} + i\mathrm{Tr}G_{0,\alpha\alpha}^{-1}G_{\alpha\alpha}\Big] + \frac{1}{2}\Gamma_2[D, G_{ss}, G_{\alpha\alpha}],
\end{aligned}
\tag{40}
$$

where we have used the full propagator of photons $D_{ij}(x,y) = \langle TA_i(x)A_j(y)\rangle$ (the brackets representing expectation values), that of dipoles in the ground state $G_{ss}(x,y) = \langle T\psi_s(x)\psi_s^*(y)\rangle$ and that of dipoles in 1st excited states $G_{\alpha\alpha}(x,y) = \langle T\psi_\alpha(x)\psi_\alpha^*(y)\rangle$ and shown the case of vanishing background fields $\langle A_i\rangle = 0$, $\langle \psi_s^{(*)}\rangle = 0$ and $\langle \psi_\alpha^{(*)}\rangle = 0$. Here, $iD_{0,ij}^{-1}$, $iG_{0,ss}^{-1}$ and $iG_{0,\alpha\alpha}^{-1}$ are written by,

$$
iD_{0,ij}^{-1}(x,y) \quad = \quad \delta_{ij}\Big(-\partial_x^2 - \delta_{Z_{ph}}\partial_x^2\Big)\delta(x-y),
\tag{41}
$$

$$
iG_{0,ss}^{-1}(x,y) \quad = \quad \left(i\frac{\partial}{\partial x^0} + \frac{\nabla_i^2}{2m} + \mu_c + \delta_{Z_s}i\frac{\partial}{\partial x^0} + \frac{\delta_{m_s^{-1}}\nabla_i^2}{2} + \delta_{\mu,s}\right)\delta(x-y),
\tag{42}
$$

$$
iG_{0,\alpha\alpha}^{-1}(x,y) \quad = \quad \left(i\frac{\partial}{\partial x^0} + \frac{\nabla_i^2}{2m} - \frac{1}{I} + \mu_c + \delta_{Z_1}i\frac{\partial}{\partial x^0} + \frac{\delta_{m_1^{-1}}\nabla_i^2}{2} - \delta_{I^{-1}} + \delta_{\mu,1st}\right)\delta(x-y).
\tag{43}
$$

We find that counter-terms are in $iD_{0,ij}$, $iG_{0,ss}^{-1}$ and $iG_{0,\alpha\alpha}^{-1}$. In 2PI effective action, the term $\frac{\Gamma_2}{2}$ represents all the 2-Particle-Irreducible loop diagrams in loop-expansion technique [53]. This term is expressed in Figure 9 for up to $O((ed_e)^4)$. We find diagrams involving counter-terms.
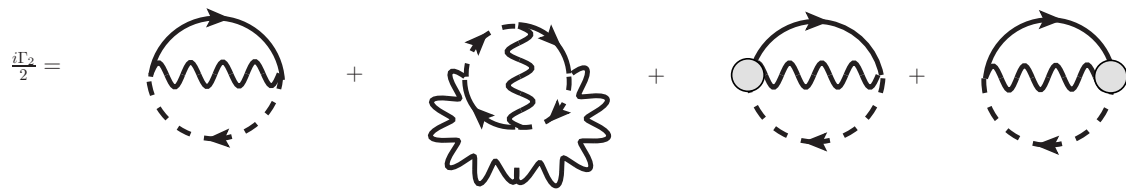
$$\frac{i\Gamma_2}{2} =$$ $+$ $+$ $+$

Figure 9. 2-Particle-Irreducible diagrams in Quantum Brain Dynamics in 3-loop order. The wavy, solid and dotted lines represent the full propagator for photons, dipoles in the ground state and dipoles in 1st excited states, respectively.

Differentiating 2PI action by propagators, we can derive the Kadanoff–Baym (KB) equations [52–54]. By the relation $\frac{\delta \Gamma_{2PI}}{\delta D} = 0$, we can derive the KB equations for photons as,

$$i\left(D_0^{-1} - \Pi \right) = iD^{-1}, \tag{44}$$

with $\Pi_{ij}(x,y) \equiv i\frac{\delta\Gamma_2}{\delta D_{ji}(y,x)}$. (Π is not renormalized due to $\delta_{Z_{ph}} = 0$.) By the relation $\frac{\delta\Gamma_{2PI}}{\delta G_{ss}} = 0$, we derive the KB equations for dipoles in the ground state as,

$$i\left(G_{0,ss}^{-1} - \Sigma_{ss} \right) = iG_{ss}^{-1}, \tag{45}$$

with $\Sigma_{ss} \equiv \frac{i}{2}\frac{\delta\Gamma_2}{\delta G_{ss}}$. In Fourier transformation in this equation, we can use the renormalized self-energy $\Sigma_{ss,\mathrm{ren}}$ as,

$$\Sigma_{ss,\mathrm{ren}}(p) = \Sigma_{ss}(p) + i\left(p^0 \delta_{Z_s} - \frac{\delta_{m_s^{-1}} \mathbf{p}^2}{2} + \delta_{\mu,s} \right), \tag{46}$$

where we adopt counter-terms derived in perturbation theory in the previous section. In the relation $\frac{\delta\Gamma_{2PI}}{\delta G_{\alpha\alpha}} = 0$, we derive the KB equations for dipoles in the 1st excited states as,

$$i\left(G_{0,\alpha\alpha}^{-1} - \Sigma_{\alpha\alpha} \right) = iG_{\alpha\alpha}^{-1}, \tag{47}$$

with $\Sigma_{\alpha\alpha} \equiv \frac{i}{2}\frac{\delta\Gamma_2}{\delta G_{\alpha\alpha}}$. Here we can use the renormalized self-energy $\Sigma_{\alpha\alpha,\mathrm{ren}}$ in Fourier transformation as,

$$\Sigma_{\alpha\alpha,\mathrm{ren}}(p) = \Sigma_{\alpha\alpha}(p) + i\left(p^0 \delta_{Z_1} - \frac{\delta_{m_1^{-1}} \mathbf{p}^2}{2} - \delta_{I^{-1}} + \delta_{\mu,1st} \right). \tag{48}$$

The right-hand side in this equation is depicted in Feynman diagrams in Figure 10. We adopt the same counter-terms as those in perturbation theory in the previous section.
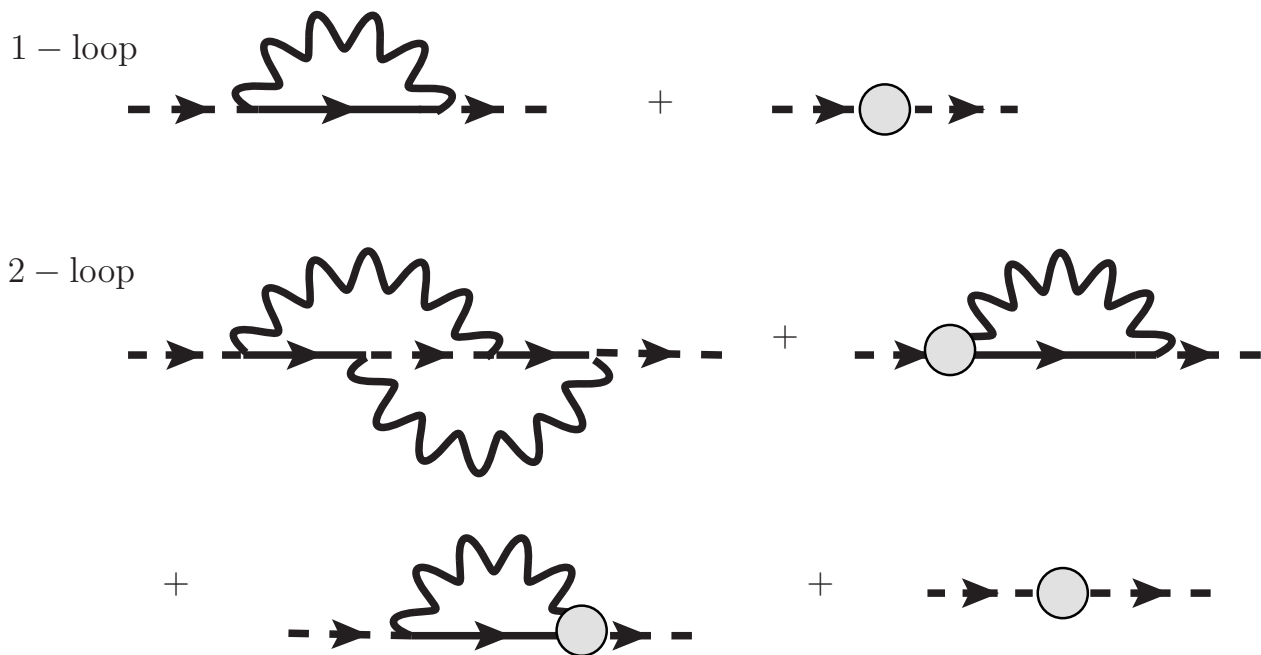
Figure 10. Self-energy for dipoles in 1st excited states in 1-loop and 2-loop orders.

5. Discussion

In this paper, we have introduced the Lagrangian density for Quantum Brain Dynamics (QBD) in $3+1$ dimensions and shown the Feynman rules for propagators, vertices and their counter-terms. We have investigated how to cancel ultra-violet (UV) divergences for 1-loop and 2-loop self-energy and 1-loop 3-point vertex corrections in the perturbation theory in the coupling expansion of ed_e. The photon self-energy has no UV divergent terms, at least in 2-loop order. The dipole self-energy involves, at most, cubic-divergent terms in 1-loop order canceled by counter-terms. The vertex corrections for 1-loop 3-point vertices involve, at most, quadratic divergent terms canceled by counter-terms. We can adopt these counter-terms derived in the perturbation theory to cancel UV divergences in the self-energy emerging in the Kadanoff–Baym (KB) equations derived in the 2-Particle-Irreducible effective action technique.

Using the counter-terms derived in this paper, we can cancel UV divergences in self-energy for dipoles in lattice simulations of the KB equations in QBD. We set the momenta $l^\mu \to \frac{2\pi n^\mu}{2a_s N_s}$ with $n^\mu = -N_s, -N_s + 1, \cdots N_s - 1, N_s$ on the lattice with lattice spacing a_s. The finite UV cutoff Λ in the integral $\int dl^0$ is then $\pm \frac{\pi}{a_s}$. We can then calculate finite counter-terms in self-energy with a finite cutoff on the lattice. Using them in numerical simulations of time-evolution of KB equations, we might find convergent behaviors in increasing the cutoff on the lattice $\frac{\pi}{a_s}$ (decreasing lattice spacing a_s). Juchem et al. [56] have reported that the convergent behaviors appear in increasing cutoff by renormalizing the non-local sunset self-energy in the ϕ^4 model in $2+1$ dimensions. Without renormalization, the numerical results of KB equations are dependent on the cutoff in ϕ^4 theory. The convergent behaviors are also expected to appear in numerical simulations in KB equations in QBD using the counter-terms derived in this paper, although we require numerical costs involving parallel computations to check the convergence since we need to trace the time-evolution of KB equations in $3+1$ dimensions during equilibration on the lattice with several cutoffs and discuss numerical results in cases with and without renormalization.

We can consider the Ward–Takahashi identity in QBD. We shall consider the case when we do not adopt axial gauge fixing conditions, such as $A^0 = 0$, but adopt Lorentz invariant gauge fixing conditions. Using electric fields written by $E_i = -\partial_i A_0 + \partial_0 A_1$ and the 4th term in the Lagrangian density in Equation (17), the Feynman rules for vertices in Figure 1 are changed by,

$$\frac{2ed_e}{\sqrt{6}}(ik^0)\left[-\alpha\left(\delta_i^1 + i\alpha\delta_i^2\right) + \sqrt{2}(1-|\alpha|)\delta_i^3\right] \quad \rightarrow \quad \frac{2ed_e}{\sqrt{6}}\left[(ik^0)\left(-\alpha\left(\delta_\mu^1 + i\alpha\delta_\mu^2\right) + \sqrt{2}(1-|\alpha|)\delta_\mu^3\right)\right.$$
$$\left.-i\delta_\mu^0\left(-\alpha\left(k^1 + i\alpha k^2\right) + \sqrt{2}(1-|\alpha|)k^3\right)\right], \quad (49)$$

and,

$$\frac{2ed_e}{\sqrt{6}}(-ik^0)\left[\alpha\left(\delta_i^1 - i\alpha\delta_i^2\right) - \sqrt{2}(1-|\alpha|)\delta_i^3\right] \quad \rightarrow \quad \frac{2ed_e}{\sqrt{6}}\left[(-ik^0)\left(\alpha\left(\delta_\mu^1 - i\alpha\delta_\mu^2\right) - \sqrt{2}(1-|\alpha|)\delta_\mu^3\right)\right.$$
$$\left.+i\delta_\mu^0\left(\alpha\left(k^1 - i\alpha k^2\right) - \sqrt{2}(1-|\alpha|)k^3\right)\right], \quad (50)$$

with subscripts of spatial coordinate $i = 1, 2, 3$ and subscripts of space-time coordinate $\mu = 0, 1, 2, 3$. We find that inner products with external momenta k^μ with the above vertices are zero. Using this property, Feynman diagrams involving inner products of vertices and momenta k^μ are zero even if the condition $k^2 = 0$ is not satisfied so we find the Ward–Takahashi identity in QBD. Using this identity, we find that the longitudinal component with $\frac{k^\mu k^\nu}{k^2}$ in propagators for photons does not contribute to physical quantities, such as the S-matrix.

We shall discuss the renormalizability in QBD in $3 + 1$ dimensions. We have investigated UV divergences in self-energy in the expansion of dipole moment $2ed_e$. Up to 2-loop order self-energy, we need not introduce new counter-terms in our Lagrangian density. However, we might need to introduce terms such as $\psi_s^* \psi_s A_i A_i$, $\psi_s^* \psi_s \psi_\alpha^* \psi_\alpha$ ($\alpha = 0, \pm 1$), and so on, in higher loop order self-energy. Similar problems will occur in Quantum Electrodynamics for non-relativistic charged bosons labeled by field $\varphi^{(*)}$ with interaction term $\partial A \varphi^* \varphi$, where we need to introduce additional φ^4 interaction terms to renormalize 4-point vertices of $\varphi^{(*)}$ appearing in $\langle(\partial A \varphi^* \varphi)^4\rangle$. In QBD, the terms such as $\psi_s^* \psi_s A_i A_i$ and ψ^4 might be introduced. If further additional terms need not emerge, we will arrive at renormalizable theory. Otherwise, the QBD Lagrangian in this paper is non-renormalizable and will represent a low-energy effective theory. We have introduced the hierarchy $k\left(\sim \frac{1}{I}\right) \ll m \ll \Lambda$ with $\frac{1}{I} = 4\,\text{meV}$, mass $m = 18 \times 940\,\text{MeV}$ for water molecules and cutoff Λ. The dipole moment $2ed_e$ times $\frac{1}{I} = 4\,\text{meV}$ (or k) is the order 10^{-7} due to elementary charge $e = 0.3$ and $d_e = 0.2 \times 10^{-10}$ m for water molecules. Then the perturbation is achieved for expansion with sufficiently small $(2ed_e/I)^n$ ($n = 2, 3, 4, \cdots$). However, if we expand by $(2ed_e\Lambda)^n$ and our QBD Lagrangian is non-renormalizable, we find that the order of Λ is 10^4 eV in $2ed_e\Lambda \sim 1$ and that QBD is effective in typical frequency $p^0 \ll \Lambda \sim 10^4$ eV. Then we need to adopt the hierarchy $\frac{1}{I} \ll \Lambda \ll 1/(2ed_e) \ll m$ with typical momenta $p^0 \ll \Lambda$. (Or we might adopt $\frac{1}{I} \ll 1/(2ed_e) \ll \Lambda \ll m$ with expansions by $\frac{\Lambda}{m}$.)

Our results will be applied to trace our decision-making or thinking processes in brain dynamics. Human decision-making is mathematically described in quantum-like theory in quantum cognition adopting quantum superposition and entanglement, which cannot be explained classically [57–62], although no physical degrees of freedom are provided in quantum cognition. QBD might provide concrete quantum degrees of freedom in quantum cognition. We adopt the theory of QBD and holography [14]. A single photon has a superposition state of two or more paths, as given by,

$$|\Phi\rangle = \sum_i |\text{path } i\rangle \rightarrow \sum_i |\text{path } i\rangle|\text{hologram } i\rangle \rightarrow \sum_i |\text{path } i\rangle|\text{hologram } i\rangle|\text{decision}i\rangle. \quad (51)$$

The photon superposition state propagating through two or more paths will provide a quantum state involving entanglement with holograms. Optical parallel information processing through holograms will provide quantum decision-making involving entanglement, as shown in the above equation. Increasing the number of photons, statistical

properties of photons propagating through holograms in water–photon system will emerge. We then encounter quantum many-body problems in a water–photon system to describe our decision-making or thinking processes. Quantum many-body properties of water dipoles and photons can be described by the KB equation in quantum field theory. We can then adopt renormalization in an interacting water–photon system to trace our thinking processes in brain dynamics using KB equations.

In canceling UV divergences emerging in self-energy and vertex corrections by renormalization, we encounter arbitrariness in finite parts in counter-terms in renormalization prescription [48]. In achieving the invariance of the theory in renormalization prescriptions, parameters $(m, 1/I, \mu_c, 2ed_e)$ will become dependent on the renormalization scale a_s (lattice spacing). The contributions from smaller scales than a_s are renormalized into those parameters, so that the coarse graining procedures cause group, namely Renormalization Group (RG). The changes in parameters for scales a_s are described by the RG equations in QBD. The RG equations describe running parameters of $(m, 1/I, \mu_c, 2ed_e)$ dependent on the renormalization scale a_s. In an increasing scale a_s with renormalizing contributions from smaller scales, we might encounter the fixed point in RG equations independent of further coarse graining procedures. The fixed point represents scale-free physical phenomena in QBD. We then find the fractality in water–photon systems representing scale-invariant physics by solving fixed-point solutions in RG equations. Furthermore, when properties larger than the momentum cutoff Λ or those smaller scales than a_s (with the momentum cutoff $\Lambda \sim \frac{1}{a_s}$) are renormalized in QBD theory, we might encounter a new effective theory in macroscopic scales from microscopic water–photon dynamics. The effective theory might provide macroscopic conscious phenomena in brain functions. Renormalization in this work will be extended to describe the diversity in multi-scale brain dynamics involving running parameters, fractality in water–photon systems and so on.

Our paper, following on from a series of previous studies [13–15], provides a basis for the proper construction of the Hamiltonian structure of the Quantum Brain Dynamics with respect to a renormalization group application that shows the cancellation of divergent terms. Importantly, the resultant Hamiltonian exhibits fractal self-similar properties that could lead to a better understanding of the quantum degrees of freedom in the human brain in a hierarchical manner. We will explore these repercussions in the context of dipole–dipole interactions within neurons in future work.

6. Concluding Remarks and Perspectives

We have introduced the Lagrangian density in QBD in $3 + 1$ dimensions and shown the counter-terms in the Lagrangian. We have derived counter-terms for the cancellation of ultra-violet (UV) divergences in self-energy and vertex corrections in perturbation theory with the coupling expansion of the dipole moment. Counter-terms will be adopted to cancel UV divergences in numerical simulations of Kadanoff–Baym equations during equilibration. Our analysis will be extended to the renormalization group (RG) method in QBD to investigate running parameters of mass, dipole moment, moment of inertia and chemical potentials and show fractal-like properties for water–photon systems in fixed points in RG equations.

Data Availability Statement: Not applicable.

Conflicts of Interest: The authors declare no conflict of interest.

Appendix A. Calculations of 1-Loop Self-Energy of Dipoles in 1st Excited States

We shall calculate self-energy in Equation (26).

For calculations of the coefficient for self-energy, we have used the relation,

$$\frac{2ed_e}{\sqrt{6}}\left[\alpha(\delta_i^1 - i\alpha\delta_i^2) - \sqrt{2}(1 - |\alpha|)\delta_i^3\right] \cdot \delta^{ij} \cdot \frac{2ed_e}{\sqrt{6}}\left[-\alpha(\delta_j^1 + i\alpha\delta_j^2) + \sqrt{2}(1 - |\alpha|)\delta_j^3\right] = -\frac{4}{3}(ed_e)^2. \tag{A1}$$

When we use $\frac{\mathbf{p}^2}{2m} \simeq \sqrt{\mathbf{p}^2 + m^2} - m$ and the relation,

$$
\begin{aligned}
&\left[p^0 + \mu_c - (\sqrt{\mathbf{p}^2 + m^2} - m - i\epsilon)\right]\left[p^0 + \mu_c + \sqrt{\mathbf{p}^2 + m^2} + m - i\epsilon\right] \\
&= \left(p^0 + \mu_c + m\right)^2 - (\sqrt{\mathbf{p}^2 + m^2} - i\epsilon)^2 \\
&= \left(p^0 + \mu_c + m\right)^2 - (\mathbf{p}^2 + m^2) + i\epsilon,
\end{aligned}
\tag{A2}
$$

in the denominator in Equation (26), we can rewrite $\Sigma_{\alpha\alpha}$ by,

$$
\begin{aligned}
\Sigma_{\alpha\alpha}(p) &\simeq -\frac{4}{3}(ed_e)^2 \int_k (k^0)^2 \frac{-\left(p^0 - k^0 + m + \mu_c + \sqrt{(\mathbf{p} - \mathbf{k})^2 + m^2}\right)}{[(p^0 - k^0 + m + \mu_c)^2 - (\mathbf{p} - \mathbf{k})^2 - m^2 + i\epsilon](k^2 + i\epsilon)} \\
&= -\frac{4}{3}(ed_e)^2 \int_k \int_0^1 dx \frac{-(k^0)^2\left(p^0 - k^0 + m + \mu_c + \sqrt{(\mathbf{p} - \mathbf{k})^2 + m^2}\right)}{[x((p^0 - k^0 + m + \mu_c)^2 - (\mathbf{p} - \mathbf{k})^2 - m^2) + (1 - x)k^2 + i\epsilon]^2},
\end{aligned}
\tag{A3}
$$

where we have used Equation (24). In the above equation, the denominator is

$$
\begin{aligned}
&x\left((p^0 - k^0 + m + \mu_c)^2 - (\mathbf{p} - \mathbf{k})^2 - m^2\right) + (1 - x)k^2 \\
&= x\left[(k^0)^2 - 2k^0(p^0 + m + \mu_c) + (p^0 + m + \mu_c)^2 - \mathbf{k}^2 + 2\mathbf{p} \cdot \mathbf{k} - \mathbf{p}^2 - m^2\right] + (1 - x)k^2 \\
&= k^2 - 2xk^0(p^0 + m + \mu_c) + x(p^0 + m + \mu_c)^2 + 2x\mathbf{p} \cdot \mathbf{k} - x\mathbf{p}^2 - xm^2 \\
&= \left(k^0 - x(p^0 + m + \mu_c)\right)^2 - (\mathbf{k} - x\mathbf{p})^2 + x(1 - x)(p^0 + m + \mu_c)^2 - x(1 - x)\mathbf{p}^2 - xm^2 \\
&= l^2 - \Delta_\alpha(p),
\end{aligned}
\tag{A4}
$$

where we have set,

$$
\begin{aligned}
l^0 &\equiv k^0 - x(p^0 + m + \mu_c), \tag{A5} \\
\mathbf{l} &\equiv \mathbf{k} - x\mathbf{p}, \tag{A6} \\
\Delta_\alpha(p) &\equiv xm^2 + x(1 - x)\mathbf{p}^2 - x(1 - x)(p^0 + m + \mu_c)^2. \tag{A7}
\end{aligned}
$$

The next step is to expand the numerator in Equation (A3). Using the hierarchy given by,

$$|\mathbf{p}| \ll m \ll |\mathbf{l}|, \tag{A8}$$

we find,

$$
\begin{aligned}
\sqrt{(\mathbf{k} - \mathbf{p})^2 + m^2} &= \sqrt{(\mathbf{l} - (1-x)\mathbf{p})^2 + m^2} \\
&= \sqrt{\mathbf{l}^2 - 2(1-x)\mathbf{l}\cdot\mathbf{p} + (1-x)^2\mathbf{p}^2 + m^2} \\
&= |\mathbf{l}|\sqrt{1 - 2(1-x)\frac{\mathbf{l}\cdot\mathbf{p}}{\mathbf{l}^2} + \frac{m^2 + (1-x)^2\mathbf{p}^2}{\mathbf{l}^2}} \\
&\simeq |\mathbf{l}|\left(1 - (1-x)\frac{\mathbf{l}\cdot\mathbf{p}}{\mathbf{l}^2} + \frac{m^2 + (1-x)^2\mathbf{p}^2}{2\mathbf{l}^2} - \frac{1}{8}\left(2(1-x)\frac{\mathbf{l}\cdot\mathbf{p}}{\mathbf{l}^2}\right)^2\right),
\end{aligned}
\tag{A9}
$$

where we have used the relation,

$$
\sqrt{1+\eta} = 1 + \frac{1}{2}\eta - \frac{1}{8}\eta^2 + \cdots.
\tag{A10}
$$

We can use,

$$
\begin{aligned}
-\left(k^0\right)^2\left(p^0 - k^0 + m + \mu_c\right) &= -\left[l^0 + x(p^0 + m + \mu_c)\right]^2\left(p^0 + m + \mu_c - l^0 - x(p^0 + m + \mu_c)\right) \\
&= -\left[\left(l^0\right)^2 + 2xl^0(p^0 + m + \mu_c) + x^2(p^0 + m + \mu_c)^2\right] \\
&\quad \times \left[(1-x)(p^0 + m + \mu_c) - l^0\right] \\
&\rightarrow -\left[\left(l^0\right)^2 + x^2(p^0 + m + \mu_c)^2\right](1-x)(p^0 + m + \mu_c) \\
&\quad + 2x\left(l^0\right)^2(p^0 + m + \mu_c) \\
&= -\left(l^0\right)^2(1 - 3x)(p^0 + m + \mu_c) - x^2(1-x)(p^0 + m + \mu_c)^3,
\end{aligned}
\tag{A11}
$$

where we have omitted odd power in l^0. We also use,

$$
\begin{aligned}
-\left(k^0\right)^2\sqrt{(\mathbf{p} - \mathbf{k})^2 + m^2} &= -\left[l^0 + x(p^0 + m + \mu_c)\right]^2 \\
&\quad \times |\mathbf{l}|\left(1 - (1-x)\frac{\mathbf{l}\cdot\mathbf{p}}{\mathbf{l}^2} + \frac{m^2 + (1-x)^2\mathbf{p}^2}{2\mathbf{l}^2} - \frac{1}{8}\left(2(1-x)\frac{\mathbf{l}\cdot\mathbf{p}}{\mathbf{l}^2}\right)^2\right) \\
&\rightarrow -\left[\left(l^0\right)^2 + x^2(p^0 + m + \mu_c)^2\right] \\
&\quad \times |\mathbf{l}|\left(1 + \frac{m^2 + (1-x)^2\mathbf{p}^2}{2\mathbf{l}^2} - \frac{(1-x)^2\mathbf{p}^2}{6\mathbf{l}^2}\right),
\end{aligned}
\tag{A12}
$$

where we have omitted the odd power of l^μ and used the relation $l^i l^j \rightarrow \frac{\mathbf{l}^2}{3}\delta^{ij}$ satisfied in the integration. Using Equations (A11) and (A12), we find the numerator in Equation (A3) is written by,

$$
\begin{aligned}
&-(k^0)^2\left(p^0 - k^0 + m + \mu_c + \sqrt{(\mathbf{p} - \mathbf{k})^2 + m^2}\right) \\
&= -\left(l^0\right)^2\left[(1 - 3x)(p^0 + m + \mu_c) + |\mathbf{l}|\left(1 + \frac{m^2 + (1-x)^2\mathbf{p}^2}{2\mathbf{l}^2} - \frac{(1-x)^2\mathbf{p}^2}{6\mathbf{l}^2}\right)\right] \\
&\quad - x^2(1-x)(p^0 + m + \mu_c)^3 - x^2(p^0 + m + \mu_c)^2|\mathbf{l}|\left(1 + \frac{m^2 + (1-x)^2\mathbf{p}^2}{2\mathbf{l}^2} - \frac{(1-x)^2\mathbf{p}^2}{6\mathbf{l}^2}\right).
\end{aligned}
\tag{A13}
$$

We use the Wick rotation shown in Figure A1 where the integrand in the complex l^0 curve falls off sufficiently rapidly. Using the rotation with $l^0 = il_E^0$ and $\mathbf{l} = \mathbf{l}_E$ for the Euclidean variable l_E^ν, we can derive,

$$\Sigma_{\alpha\alpha} = -\frac{4i}{3}(ed_e)^2 \int_0^1 dx \int_{l_E} \frac{[\text{numerator 0}]}{(l_E^2 + \Delta_\alpha(p))^2}, \tag{A14}$$

with,

$$
\begin{aligned}
[\text{numerator 0}] = {} & (l_E^0)^2 \left[|\mathbf{l}_E| + (1-3x)\left(m + p^0 + \mu_c\right) + \frac{(1-x)^2\mathbf{p}^2 + m^2}{2|\mathbf{l}_E|} - \frac{(1-x)^2\mathbf{p}^2}{6|\mathbf{l}_E|} \right] \\
& - x^2 |\mathbf{l}_E| \left(m + p^0 + \mu_c\right)^2 - x^2(1-x)\left(m + p^0 + \mu_c\right)^3,
\end{aligned} \tag{A15}
$$

where we neglected terms without UV divergences. Adopting the hierarchy in non-relativistic cases given by,

$$p^0, \ \mu_c, \ \frac{\mathbf{p}^2}{2m}, \ \frac{1}{I} \ll m \ll |l^0|, |\mathbf{l}|, \tag{A16}$$

we can expand $\Delta_\alpha(p)$ in Equation (A7) as,

$$
\begin{aligned}
\Delta_\alpha(p) &= xm^2 + x(1-x)\mathbf{p}^2 - x(1-x)(p^0 + m + \mu_c)^2 \\
&\simeq -x(1-x)\left(m^2 + 2m(p^0 + \mu_c)\right) + xm^2 + x(1-x)\mathbf{p}^2 \\
&= x^2 m^2 - 2mx(1-x)\left(p^0 + \mu_c - \frac{\mathbf{p}^2}{2m}\right),
\end{aligned} \tag{A17}
$$

and use the relation,

$$
\begin{aligned}
\frac{1}{(l_E^2 + \Delta_\alpha)^2} &= \frac{1}{(l_E^2 + x^2 m^2)^2 \left(1 - \frac{2mx(1-x)\left(p^0 + \mu_c - \frac{\mathbf{p}^2}{2m}\right)}{(l_E^2 + x^2 m^2)}\right)^2} \\
&= \frac{1}{(l_E^2 + x^2 m^2)^2} \cdot \left(1 + \frac{4mx(1-x)\left(p^0 + \mu_c - \frac{\mathbf{p}^2}{2m}\right)}{(l_E^2 + x^2 m^2)}\right).
\end{aligned} \tag{A18}
$$

Using the above relation and the hierarchy in Equation (A16) for Equation (A15), we arrive at,

$$\Sigma_{\alpha\alpha}(p) = -\frac{4i}{3}(ed_e)^2 \int_0^1 dx \int_{l_E} \frac{[\text{numerator 1}]}{(l_E^2 + x^2 m^2)^2}, \tag{A19}$$

with,

$$
\begin{aligned}
[\text{numerator 1}] = {} & (l_E^0)^2 \left[|\mathbf{l}_E| + (1-3x)\left(m + p^0 + \mu_c\right) + \frac{(1-x)^2\mathbf{p}^2 + m^2}{2|\mathbf{l}_E|} - \frac{(1-x)^2\mathbf{p}^2}{6|\mathbf{l}_E|} \right] \\
& - x^2 |\mathbf{l}_E| m \left(m + 2\left(p^0 + \mu_c\right)\right) - x^2(1-x)m^2 \left(m + 3\left(p^0 + \mu_c\right)\right) \\
& + \frac{4mx(1-x)}{l_E^2 + x^2 m^2}\left((1-3x)(l_E^0)^2 m + (l_E^0)^2|\mathbf{l}_E|\right)\left(p^0 + \mu_c - \frac{\mathbf{p}^2}{2m}\right).
\end{aligned} \tag{A20}
$$

Figure A1. Wick rotation with the contour of the l^0 rotation in the complex plane. Crossed lines represent the positions of poles.

Appendix B. Calculations of 1-Loop 3-Point Vertex

We calculate 1-loop 3-point vertex in Equation (33).

We shall define $F(\alpha)$ by,

$$
\begin{aligned}
F(\alpha) &\equiv \sum_{\beta} \left(-il^0\right)^2 ik^0 \delta^{jn} \left[\beta\left(\delta_j^1 - i\beta\delta_j^2\right) - \sqrt{2}(1-|\beta|)\delta_j^3\right] \\
&\quad \times \left[\alpha\left(\delta_n^1 - i\alpha\delta_n^2\right) - \sqrt{2}(1-|\alpha|)\delta_n^3\right]\left[-\beta\left(\delta_i^1 + i\beta\delta_i^2\right) + \sqrt{2}(1-|\beta|)\delta_i^3\right] \\
&= -\left(l^0\right)^2 ik^0 \sum_{\beta}\left[\alpha\beta - \alpha^2\beta^2 + 2(1-|\alpha|)(1-|\beta|)\right] \\
&\quad \times \left[-\beta\left(\delta_i^1 + i\beta\delta_i^2\right) + \sqrt{2}(1-|\beta|)\delta_i^3\right].
\end{aligned}
\tag{A21}
$$

Since the factor $\alpha\beta - \alpha^2\beta^2 + 2(1-|\alpha|)(1-|\beta|)$ is nonzero only in cases with $\alpha = -\beta = 1$, $\alpha = -\beta = -1$ and $\alpha = \beta = 0$, namely $\alpha = -\beta$, we find the relation,

$$
F(\alpha) = -2(l^0)^2(-ik^0)\left[\alpha(\delta_i^1 - i\alpha\delta_i^2) - \sqrt{2}(1-|\alpha|)\delta_i^3\right].
\tag{A22}
$$

The factor $(-ik^0)(\alpha(\delta_i^1 - i\alpha\delta_i^2) - \sqrt{2}(1-|\alpha|)\delta_i^3)$ is found to emerge in 1-loop correction for 3-point vertex.

Then the δ_{ed_e} in counter-term for 1-loop correction is derived as,

$$
\begin{aligned}
-\frac{2\delta_{ed_e}}{\sqrt{6}} &= -2\left(\frac{2ed_e}{\sqrt{6}}\right)^3 \int_l \left(l^0\right)^2 \frac{i}{l^2 + i\epsilon} \\
&\quad \times \frac{i}{p^0 + l^0 - \frac{(\mathbf{p+l})^2}{2m} - \frac{1}{l} + \mu_c + i\epsilon} \times \frac{i}{p^0 + l^0 + k^0 - \frac{(\mathbf{p+l+k})^2}{2m} + \mu_c + i\epsilon}.
\end{aligned}
\tag{A23}
$$

The δ_{ed_e} can be rewritten by,

$$
\begin{aligned}
-\frac{2\delta_{ed_e}}{\sqrt{6}} &\simeq -2\left(\frac{2ed_e}{\sqrt{6}}\right)^3 \int_l \left(l^0\right)^2 \frac{i}{l^2 + i\epsilon} \\
&\quad \times \frac{i\left(p^0 + l^0 + \sqrt{(\mathbf{p+l})^2 + m^2} + m + \mu_c - \frac{1}{l}\right)}{\left(p^0 + l^0 + m + \mu_c - \frac{1}{l}\right)^2 - \left((\mathbf{p+l})^2 + m^2\right) + i\epsilon} \\
&\quad \times \frac{i\left(p^0 + l^0 + k^0 + \sqrt{(\mathbf{p+l+k})^2 + m^2} + m + \mu_c\right)}{(p^0 + l^0 + k^0 + m + \mu_c)^2 - \left((\mathbf{p+l+k})^2 + m^2\right) + i\epsilon} \\
&= -2\left(\frac{2ed_e}{\sqrt{6}}\right)^3 \int_l i^3 2! \int_0^1 dx \int_0^1 dy \times \frac{[\text{numerator 3}]}{[\text{denominator 3}]},
\end{aligned}
\tag{A24}
$$

where we set,

$$
\begin{aligned}
[\text{numerator 3}] \;=\; & \left(p^0 + l^0 + \sqrt{(\mathbf{p}+\mathbf{l})^2 + m^2} + m + \mu_c - \frac{1}{I} \right) \\
& \times \left(p^0 + l^0 + k^0 + \sqrt{(\mathbf{p}+\mathbf{l}+\mathbf{k})^2 + m^2} + m + \mu_c \right) \times \left(l^0 \right)^2,
\end{aligned}
\tag{A25}
$$

and,

$$
\begin{aligned}
[\text{denominator 3}] \;=\; & \left((1-x-y)l^2 + x\left[\left(p^0 + l^0 + m + \mu_c - \frac{1}{I} \right)^2 - \left((\mathbf{p}+\mathbf{l})^2 + m^2 \right) \right] \right. \\
& \left. + y\left[\left(p^0 + l^0 + k^0 + m + \mu_c \right)^2 - \left((\mathbf{p}+\mathbf{l}+\mathbf{k})^2 + m^2 \right) \right] + i\epsilon \right)^3,
\end{aligned}
\tag{A26}
$$

and we have used Feynman's formula given by,

$$
\frac{1}{ABC} = \int_0^1 dx \int_0^1 dy \frac{2!}{\left((1-x-y)A + xB + yC \right)^3}.
\tag{A27}
$$

The inside of the bracket of denominator 3 is expanded as,

$$
\begin{aligned}
& (1-x-y)l^2 + x\left[\left(p^0 + l^0 + m + \mu_c - \frac{1}{I} \right)^2 - \left((\mathbf{p}+\mathbf{l})^2 + m^2 \right) \right] \\
& + y\left[\left(p^0 + l^0 + k^0 + m + \mu_c \right)^2 - \left((\mathbf{p}+\mathbf{l}+\mathbf{k})^2 + m^2 \right) \right] \\
=\; & (1-x-y)\left((l^0)^2 - \mathbf{l}^2 \right) \\
& + x\left[(l^0)^2 + 2l^0\left(p^0 + m + \mu_c - \frac{1}{I} \right) + \left(p^0 + m + \mu_c - \frac{1}{I} \right)^2 - \mathbf{l}^2 - 2\mathbf{p}\cdot\mathbf{l} - \mathbf{p}^2 - m^2 \right] \\
& + y\left[(l^0)^2 + 2l^0\left(p^0 + k^0 + m + \mu_c \right) + \left(p^0 + k^0 + m + \mu_c \right)^2 \right. \\
& \left. - \mathbf{l}^2 - 2(\mathbf{p}+\mathbf{k})\cdot\mathbf{l} - (\mathbf{p}+\mathbf{k})^2 - m^2 \right] \\
=\; & \left(l^0 \right)^2 + 2l^0\left[x\left(p^0 + m + \mu_c - \frac{1}{I} \right) + y\left(p^0 + k^0 + m + \mu_c \right) \right] - \mathbf{l}^2 - 2\mathbf{l}\cdot(x\mathbf{p} + y(\mathbf{p}+\mathbf{k})) \\
& + x\left(p^0 + m + \mu_c - \frac{1}{I} \right)^2 - x(\mathbf{p}^2 + m^2) + y\left(p^0 + k^0 + m + \mu_c \right)^2 - y\left[(\mathbf{p}+\mathbf{k})^2 + m^2 \right] \\
=\; & \left(q^0 \right)^2 - \left[x\left(p^0 + m + \mu_c - \frac{1}{I} \right) + y\left(p^0 + k^0 + m + \mu_c \right) \right]^2 \\
& - \mathbf{q}^2 + (x\mathbf{p} + y(\mathbf{p}+\mathbf{k}))^2 \\
& + x\left(p^0 + m + \mu_c - \frac{1}{I} \right)^2 - x(\mathbf{p}^2 + m^2) + y\left(p^0 + k^0 + m + \mu_c \right)^2 - y\left[(\mathbf{p}+\mathbf{k})^2 + m^2 \right] \\
=\; & q^2 - \Delta,
\end{aligned}
\tag{A28}
$$

where we set q^0 and $\mathbf{q}$ as,

$$
\begin{aligned}
q^0 \;=\; & l^0 + x\left(p^0 + m + \mu_c - \frac{1}{I} \right) + y\left(p^0 + k^0 + m + \mu_c \right),
\end{aligned}
\tag{A29}
$$

$$
\mathbf{q} \;=\; \mathbf{l} + x\mathbf{p} + y(\mathbf{p}+\mathbf{k}),
\tag{A30}
$$

$$
\int_l \;\rightarrow\; \int_q
\tag{A31}
$$

and define Δ as,

$$
\begin{aligned}
\Delta \equiv \ & (x+y)m^2 - 2xy\mathbf{p} \cdot (\mathbf{p}+\mathbf{k}) + y(1-y)(\mathbf{p}+\mathbf{k})^2 + x(1-x)\mathbf{p}^2 \\
& + 2xy\left(p^0 + m + \mu_c - \frac{1}{I}\right)\left(p^0 + k^0 + m + \mu_c\right) \\
& -x(1-x)\left(p^0 + m + \mu_c - \frac{1}{I}\right)^2 - y(1-y)\left(p^0 + k^0 + m + \mu_c\right)^2.
\end{aligned}
\tag{A32}
$$

Next, we calculate numerator 3. Using Equation (A29), we can write,

$$
\begin{aligned}
p^0 + l^0 &= q^0 + (1-x-y)p^0 - x\left(m + \mu_c - \frac{1}{I}\right) - y(k^0 + m + \mu_c), \\
p^0 + l^0 + k^0 &= q^0 + (1-x-y)p^0 - x\left(m + \mu_c - \frac{1}{I}\right) + (1-y)k^0 - y(m + \mu_c).
\end{aligned}
\tag{A33}
$$

Using Equation (A30), we find the relations,

$$
\begin{aligned}
(\mathbf{p}+\mathbf{l})^2 + m^2 &= (\mathbf{q} - x\mathbf{p} - y(\mathbf{p}+\mathbf{k}) + \mathbf{p})^2 + m^2 \\
&= \mathbf{q}^2 + 2\mathbf{q} \cdot [(1-x-y)\mathbf{p} - y\mathbf{k}] + [(1-x-y)\mathbf{p} - y\mathbf{k}]^2 + m^2
\end{aligned}
\tag{A34}
$$

$$
\begin{aligned}
\sqrt{(\mathbf{p}+\mathbf{l})^2 + m^2} \simeq \ & |\mathbf{q}| + \frac{2\mathbf{q} \cdot [(1-x-y)\mathbf{p} - y\mathbf{k}] + [(1-x-y)\mathbf{p} - y\mathbf{k}]^2 + m^2}{2|\mathbf{q}|} \\
& -\frac{1}{8}\frac{(2\mathbf{q} \cdot [(1-x-y)\mathbf{p} - y\mathbf{k}])^2}{|\mathbf{q}|^3},
\end{aligned}
\tag{A35}
$$

where we have used relation $|\mathbf{p}|, |\mathbf{k}| \ll m \ll |\mathbf{q}|$ and Equation (A10). Similarly, we find the relation,

$$
\begin{aligned}
(\mathbf{p}+\mathbf{l}+\mathbf{k})^2 + m^2 &= (\mathbf{q} - x\mathbf{p} - y(\mathbf{p}+\mathbf{k}) + \mathbf{p} + \mathbf{k})^2 + m^2 \\
&= \mathbf{q}^2 + 2\mathbf{q} \cdot [(1-x-y)\mathbf{p} + (1-y)\mathbf{k}] + [(1-x-y)\mathbf{p} + (1-y)\mathbf{k}]^2 + m^2
\end{aligned}
\tag{A36}
$$

$$
\begin{aligned}
\sqrt{(\mathbf{p}+\mathbf{l}+\mathbf{k})^2 + m^2} \simeq \ & |\mathbf{q}| + \frac{2\mathbf{q} \cdot [(1-x-y)\mathbf{p} + (1-y)\mathbf{k}] + [(1-x-y)\mathbf{p} + (1-y)\mathbf{k}]^2 + m^2}{2|\mathbf{q}|} \\
& -\frac{1}{8}\frac{(2\mathbf{q} \cdot [(1-x-y)\mathbf{p} + (1-y)\mathbf{k}])^2}{|\mathbf{q}|^3}.
\end{aligned}
\tag{A37}
$$

Using Equations (A29), (A33), (A35) and (A37), numerator 3 in Equation (A25) is rewritten by,

$$
\begin{aligned}
\text{[numetator 3]} \quad = \quad & \left(q^0 + (1-x-y)p^0 - x\left(m + \mu_c - \frac{1}{I} \right) - y\left(k^0 + m + \mu_c \right) \right. \\
& + |\mathbf{q}| + \frac{2\mathbf{q} \cdot [(1-x-y)\mathbf{p} - y\mathbf{k}] + ((1-x-y)\mathbf{p} - y\mathbf{k})^2 + m^2}{2|\mathbf{q}|} \\
& \left. - \frac{1}{8} \frac{(2\mathbf{q} \cdot [(1-x-y)\mathbf{p} - y\mathbf{k}])^2}{|\mathbf{q}|^3} + m + \mu_c - \frac{1}{I} \right) \\
& \times \left(q^0 + (1-x-y)p^0 - x\left(m + \mu_c - \frac{1}{I} \right) - y(m + \mu_c) + (1-y)k^0 \right. \\
& + |\mathbf{q}| + \frac{2\mathbf{q} \cdot [(1-x-y)\mathbf{p} + (1-y)\mathbf{k}] + ((1-x-y)\mathbf{p} + (1-y)\mathbf{k})^2 + m^2}{2|\mathbf{q}|} \\
& \left. - \frac{1}{8} \frac{(2\mathbf{q} \cdot [(1-x-y)\mathbf{p} + (1-y)\mathbf{k}])^2}{|\mathbf{q}|^3} + m + \mu_c \right) \\
& \times \left(q^0 - x\left(p^0 + m + \mu_c - \frac{1}{I} \right) - y\left(p^0 + k^0 + m + \mu_c \right) \right)^2.
\end{aligned}
\tag{A38}
$$

We shall set the renormalization point as,

$$
p^0 = -\mu_c, \quad \mathbf{p} = \mathbf{0},
\tag{A39}
$$

$$
k^0 = \frac{1}{I}, \quad |\mathbf{k}| = \frac{1}{I}.
\tag{A40}
$$

We then expand Equation (A32) in denominator 3 at the point as,

$$
\begin{aligned}
\Delta \quad = \quad & (x+y)m^2 + y(1-y)\frac{1}{I^2} + 2xy\left(m - \frac{1}{I} \right)\left(m + \frac{1}{I} \right) \\
& - x(1-x)\left(m - \frac{1}{I} \right)^2 - y(1-y)\left(m + \frac{1}{I} \right)^2 \\
= \quad & (x+y)m^2 - y(1-y)\left(m^2 + \frac{2m}{I} \right) + 2xy\left(m^2 - \frac{1}{I^2} \right) - x(1-x)\left(\frac{1}{I^2} - \frac{2m}{I} + m^2 \right) \\
= \quad & (x+y)^2 m^2 - y(1-y)\frac{2m}{I} - 2xy\frac{1}{I^2} - x(1-x)\left(-\frac{2m}{I} + \frac{1}{I^2} \right).
\end{aligned}
\tag{A41}
$$

We also expand numerator 3 in Equation (A38) at the renormalization point as,

$$
\begin{aligned}
\text{[numerator 3]} \quad = \quad & \left[q^0 + (1-x-y)(-\mu_c) - x\left(m + \mu_c - \frac{1}{I} \right) - y\left(\frac{1}{I} + m + \mu_c \right) \right. \\
& \left. + m + \mu_c - \frac{1}{I} + |\mathbf{q}| + \frac{-2y\mathbf{q} \cdot \mathbf{k} + y^2\mathbf{k}^2 + m^2}{2|\mathbf{q}|} - \frac{(2\mathbf{q} \cdot (-y\mathbf{k}))^2}{8|\mathbf{q}|^3} \right] \\
& \times \left[q^0 + (1-x-y)(-\mu_c) - x\left(m + \mu_c - \frac{1}{I} \right) - y(m + \mu_c) + (1-y)\frac{1}{I} \right. \\
& \left. + m + \mu_c + |\mathbf{q}| + \frac{2(1-y)\mathbf{q} \cdot \mathbf{k} + (1-y)^2\mathbf{k}^2 + m^2}{2|\mathbf{q}|} - \frac{(2\mathbf{q} \cdot ((1-y)\mathbf{k}))^2}{8|\mathbf{q}|^3} \right] \\
& \times \left[q^0 - x\left(m - \frac{1}{I} \right) - y\left(m + \frac{1}{I} \right) \right]^2.
\end{aligned}
\tag{A42}
$$

Due to $\mathbf{k}^2 = \frac{1}{I^2}$, we find,

$$
\text{[numerator 3]} = \left[q^0 + (1-x-y)m - (1-x+y)\frac{1}{I} + |\mathbf{q}| + \frac{-y\mathbf{q}\cdot\mathbf{k} + \frac{y^2}{2I^2} + \frac{m^2}{2}}{|\mathbf{q}|} - \frac{y^2(\mathbf{q}\cdot\mathbf{k})^2}{2|\mathbf{q}|^3} \right]
$$

$$
\times \left[q^0 + (1-x-y)m + (1+x-y)\frac{1}{I} + |\mathbf{q}| + \frac{(1-y)\mathbf{q}\cdot\mathbf{k} + \frac{(1-y)^2}{2I^2} + \frac{m^2}{2}}{|\mathbf{q}|} \right.
$$

$$
\left. - \frac{(1-y)^2(\mathbf{q}\cdot\mathbf{k})^2}{2|\mathbf{q}|^3} \right]
$$

$$
\times \left[(q^0)^2 - 2q^0\left((x+y)m + (y-x)\frac{1}{I} \right) + \left((x+y)m + (y-x)\frac{1}{I} \right)^2 \right]. \tag{A43}
$$

Neglecting the odd power of q^0 and $\mathbf{q}$ and removing finite contributions in the integral $\int_q$, we find,

$$
\text{[numerator 3]} \;\rightarrow\; (q^0)^2\left[(q^0)^2 + \left((x+y)m + (y-x)\frac{1}{I} \right)^2 \right]
$$

$$
+ q^0\left[2(1-x-y)m + 2(x-y)\frac{1}{I} + 2|\mathbf{q}| \right](-2q^0)\left[(x+y)m + (y-x)\frac{1}{I} \right]
$$

$$
+ \left[|\mathbf{q}|^2 + |\mathbf{q}|\left(2(1-x-y)m + 2(x-y)\frac{1}{I} \right. \right.
$$

$$
\left. \left. + \frac{1}{|\mathbf{q}|}\left(m^2 + \frac{y^2+(1-y)^2}{2I^2} - \frac{(y^2+(1-y)^2)(\mathbf{q}\cdot\mathbf{k})^2}{2|\mathbf{q}|^2} \right) \right) \right]
$$

$$
\times \left[(q^0)^2 + \left((x+y)m + (y-x)\frac{1}{I} \right)^2 \right]
$$

$$
+ \left[(1-x-y)m - (1-x+y)\frac{1}{I} + \frac{-y\mathbf{q}\cdot\mathbf{k}}{|\mathbf{q}|} \right]
$$

$$
\times \left[(1-x-y)m + (1+x-y)\frac{1}{I} + \frac{(1-y)\mathbf{q}\cdot\mathbf{k}}{|\mathbf{q}|} \right](q^0)^2. \tag{A44}
$$

Neglecting the anti-symmetric term for interchange of x and y and using $q^i q^j \rightarrow \frac{|\mathbf{q}|^2 \delta^{ij}}{3}$, we find,

$$
\text{[numerator 3]} \quad \rightarrow \quad (q^0)^2\left[(q^0)^2 + (x+y)^2 m^2 + (y-x)^2\frac{1}{I^2}\right]
$$

$$
-4(q^0)^2\left[(x+y)m + (y-x)\frac{1}{I}\right]\left[m - (x+y)m + (x-y)\frac{1}{I} + |\mathbf{q}|\right]
$$

$$
+(q^0)^2\left[|\mathbf{q}|^2 + 2|\mathbf{q}|(1-x-y)m + \frac{y^2 + (1-y)^2}{3I^2} + m^2\right]
$$

$$
+|\mathbf{q}|^2\left[(x+y)^2 m^2 + (y-x)^2\frac{1}{I^2}\right]
$$

$$
+(q^0)^2\left[(1-x-y)^2 m^2 - 2y(1-x-y)\frac{m}{I} - \left[(1-x)^2 - y^2\right]\frac{1}{I^2} - \frac{y(1-y)}{3I^2}\right]
$$

$$
\rightarrow \quad (q^0)^2\left[(q^0)^2 + (x+y)^2 m^2 + (y-x)^2\frac{1}{I^2}\right.
$$

$$
-4\left[(x+y)m^2 - (x+y)^2 m^2 + (x+y)m|\mathbf{q}| - (y-x)^2\frac{1}{I^2}\right]
$$

$$
+|\mathbf{q}|^2 + 2|\mathbf{q}|m(1-x-y) + \frac{y^2 + (1-y)^2}{3I^2} + m^2
$$

$$
\left. +(x+y)^2 m^2 - 2(x+y)m^2 + m^2 - 2y(1-x-y)\frac{m}{I} - \frac{(1-x)^2 - y^2}{I^2} - \frac{y(1-y)}{3I^2}\right]
$$

$$
+|\mathbf{q}|^2\left[(x+y)^2 m^2 + (y-x)^2\frac{1}{I^2}\right]. \tag{A45}
$$

As a result, we arrive at,

$$
\text{[numerator 3]} \quad \rightarrow \quad (q^0)^2\left[(q^0)^2 + |\mathbf{q}|^2 + 6m^2(x+y)(x+y-1) + 2m|\mathbf{q}|(1 - 3(x+y)) + 2m^2\right.
$$

$$
\left. + \frac{1}{I^2}\left(5(y-x)^2 + \frac{3y^2 - 3y + 1}{3} - \left((1-x)^2 - y^2\right) - 2y(1-x-y)mI\right)\right]
$$

$$
+|\mathbf{q}|^2\left((x+y)^2 m^2 + (y-x)^2\frac{1}{I^2}\right). \tag{A46}
$$

Finally, we perform the Wick rotation $q^0 = iq_E$, $\mathbf{q} = \mathbf{q}_E$ and adopt the following procedure for Equation (A41),

$$
\frac{-1}{(q_E^2 + \Delta)^3} = \frac{-1}{\left[\left(q_E^2 + (x+y)^2 m^2\right)\left(1 + \frac{\frac{x^2 - x - 2xy}{I^2} - \frac{2m}{I}(x(1-x) - y(1-y))}{q_E^2 + (x+y)^2 m^2}\right)\right]^3}
$$

$$
\rightarrow \frac{-1}{\left[q_E^2 + (x+y)^2 m^2\right]^3}\left[1 - \frac{\frac{3}{I^2}(x(x-1) - 2xy)}{q_E^2 + (x+y)^2 m^2}\right]. \tag{A47}
$$

Using the above relation and Equation (A46), Equation (A24) can be rewritten as,

$$
\begin{aligned}
-\frac{2\delta_{ed_e}}{\sqrt{6}} \;=\; & -4\left(\frac{2ed_e}{\sqrt{6}}\right)^3 \int_0^1 dx \int_0^1 dy \int_{q_E} \frac{-1}{(q_E^2 + (x+y)^2 m^2)^3} \\
& \times \left[(q_E^0)^2 \left[(q_E^0)^2 - \left(|\mathbf{q}_E|^2 + 6m^2(x+y)(x+y-1) + 2m|\mathbf{q}|(1 - 3(x+y)) + 2m^2 \right.\right.\right. \\
& \left.\left.\left. + \frac{1}{I^2}\left(5(y-x)^2 + \frac{3y^2 - 3y + 1}{3} - \left((1-x)^2 - y^2 \right) - 2y(1-x-y)mI \right) \right) \right] \right. \\
& \left. + |\mathbf{q}_E^2| \left[(x+y)^2 m^2 + \frac{(y-x)^2}{I^2} \right] \right. \\
& \left. - (q_E^0)^2 \left((q_E^0)^2 - |\mathbf{q}_E|^2 \right) \frac{\frac{3}{I^2}(x^2 - x - 2xy)}{q_E^2 + (x+y)^2 m^2} \right].
\end{aligned}
\tag{A48}
$$

References

1. Nicholls, J.G.; Martin, A.R.; Wallace, B.G.; Fuchs, P.A. *From Neuron to Brain*; Sinauer Associates Sunderland: Sunderland, MA, USA, 2001; Volume 271.
2. Hameroff, S.; Penrose, R. Orchestrated reduction of quantum coherence in brain microtubules: A model for consciousness. *Math. Comput. Simul.* **1996**, *40*, 453–480. [CrossRef]
3. Hameroff, S.; Penrose, R. Consciousness in the universe: A review of the 'Orch OR'theory. *Phys. Life Rev.* **2014**, *11*, 39–78. [CrossRef] [PubMed]
4. Kalra, A.P.; Benny, A.; Travis, S.M.; Zizzi, E.A.; Morales-Sanchez, A.; Oblinsky, D.G.; Craddock, T.J.; Hameroff, S.R.; MacIver, M.B.; Tuszynski, J.A.; et al. Electronic Energy Migration in Microtubules. *arXiv* **2022**, arXiv:2208.10628.
5. Pockett, S. Field theories of consciousness. *Scholarpedia* **2013**, *8*, 4951. [CrossRef]
6. McFadden, J. The CEMI field theory closing the loop. *J. Conscious. Stud.* **2013**, *20*, 153–168.
7. Jibu, M.; Yasue, K. The basic of quantum brain dynamics. In*Rethinking Neural Networks: Quantum Fields Biological Data*; Pribram, K.H., Ed.; Psychology Press: London, UK, 1993; pp. 121–145.
8. Vitiello, G. Dissipation and memory capacity in the quantum brain model. *Int. J. Mod. Phys. B* **1995**, *9*, 973–989. [CrossRef]
9. Hennessy, M.; Hamblin, M.R. Photobiomodulation and the brain: A new paradigm. *J. Opt.* **2016**, *19*, 013003. [CrossRef]
10. Dompe, C.; Moncrieff, L.; Matys, J.; Grzech-Leśniak, K.; Kocherova, I.; Bryja, A.; Bruska, M.; Dominiak, M.; Mozdziak, P.; Skiba, T.H.I.; et al. Photobiomodulation—underlying mechanism and clinical applications. *J. Clin. Med.* **2020**, *9*, 1724. [CrossRef]
11. Anastassiou, C.A.; Montgomery, S.M.; Barahona, M.; Buzsáki, G.; Koch, C. The effect of spatially inhomogeneous extracellular electric fields on neurons. *J. Neurosci.* **2010**, *30*, 1925–1936. [CrossRef]
12. Stuart, C.; Takahashi, Y.; Umezawa, H. On the stability and non-local properties of memory. *J. Theor. Biol.* **1978**, *71*, 605–618. [CrossRef]
13. Nishiyama, A.; Tanaka, S.; Tuszynski, J.A. Non-equilibrium Quantum Brain Dynamics II: Formulation in 3+1 dimensions. *Phys. A Stat. Mech. Its Appl.* **2021**, *567*, 125706. [CrossRef]
14. Nishiyama, A.; Tanaka, S.; Tuszynski, J.A. Quantum Brain Dynamics and Holography. *Dynamics* **2022**, *2*, 187–218. [CrossRef]
15. Nishiyama, A.; Tanaka, S.; Tuszynski, J.A. Non-Equilibrium ϕ^4 Theory in a Hierarchy: Towards Manipulating Holograms in Quantum Brain Dynamics. *Dynamics* **2023**, *3*, 1–17. [CrossRef]
16. Tegmark, M. Importance of quantum decoherence in brain processes. *Phys. Rev. E* **2000**, *61*, 4194. [CrossRef]
17. Lambert, N.; Chen, Y.N.; Cheng, Y.C.; Li, C.M.; Chen, G.Y.; Nori, F. Quantum biology. *Nat. Phys.* **2013**, *9*, 10–18. [CrossRef]
18. Kerskens, C.M.; Pérez, D.L. Experimental indications of non-classical brain functions. *J. Phys. Commun.* **2022**, *6*, 105001. [CrossRef]
19. Jibu, M.; Yasue, K. *Quantum Brain Dynamics and Consciousness*; John Benjamins: Amsterdam, The Netherlands, 1995.
20. Vitiello, G. *My Double Unveiled: The Dissipative Quantum Model of Brain*; John Benjamins Publishing: Amsterdam, The Netherlands 2001; Volume 32.
21. Sabbadini, S.A.; Vitiello, G. Entanglement and Phase-Mediated Correlations in Quantum Field Theory. Application to Brain-Mind States. *Appl. Sci.* **2019**, *9*, 3203. [CrossRef]
22. Ricciardi, L.M.; Umezawa, H. Brain and physics of many-body problems. *Kybernetik* **1967**, *4*, 44–48. [CrossRef]
23. Stuart, C.; Takahashi, Y.; Umezawa, H. Mixed-system brain dynamics: Neural memory as a macroscopic ordered state. *Found. Phys.* **1979**, *9*, 301–327. [CrossRef]
24. Fröhlich, H. Bose condensation of strongly excited longitudinal electric modes. *Phys. Lett. A* **1968**, *26*, 402–403. [CrossRef]

25. Fröhlich, H. Long-range coherence and energy storage in biological systems. *Int. J. Quantum Chem.* **1968**, *2*, 641–649. [CrossRef]

26. Davydov, A.; Kislukha, N. Solitons in One-Dimensional Molecular Chains. *Phys. Status Solidi (b)* **1976**, *75*, 735–742. [CrossRef]

27. Tuszyński, J.; Paul, R.; Chatterjee, R.; Sreenivasan, S. Relationship between Fröhlich and Davydov models of biological order. *Phys. Rev. A* **1984**, *30*, 2666. [CrossRef]

28. Del Giudice, E.; Doglia, S.; Milani, M.; Vitiello, G. Spontaneous symmetry breakdown and boson condensation in biology. *Phys. Lett. A* **1983**, *95*, 508–510. [CrossRef]

29. Del Giudice, E.; Doglia, S.; Milani, M.; Vitiello, G. A quantum field theoretical approach to the collective behaviour of biological systems. *Nucl. Phys. B* **1985**, *251*, 375–400. [CrossRef]

30. Del Giudice, E.; Preparata, G.; Vitiello, G. Water as a free electric dipole laser. *Phys. Rev. Lett.* **1988**, *61*, 1085. [CrossRef]

31. Del Giudice, E.; Smith, C.; Vitiello, G. Magnetic Flux Quantization and Josephson Systems. *Phys. Scr.* **1989**, *40*, 786–791. [CrossRef]

32. Jibu, M.; Yasue, K. A physical picture of Umezawa's quantum brain dynamics. *Cybern. Syst. Res.* **1992**, *92*, 797–804.

33. Jibu, M.; Yasue, K. Intracellular quantum signal transfer in Umezawa's quantum brain dynamics. *Cybern. Syst.* **1993**, *24*, 1–7. [CrossRef]

34. Jibu, M.; Hagan, S.; Hameroff, S.R.; Pribram, K.H.; Yasue, K. Quantum optical coherence in cytoskeletal microtubules: Implications for brain function. *Biosystems* **1994**, *32*, 195–209. [CrossRef]

35. Pribram, K.H. *Languages of the Brain: Experimental Paradoxes and Principles in Neuropsychology*; Prentice-Hall: Hoboken, NJ, USA, 1971.

36. Pribram, K.H.; Yasue, K.; Jibu, M. *Brain and Perception: Holonomy and Structure in Figural Processing*; Psychology Press: London, UK, 1991.

37. Jibu, M.; Yasue, K. What is mind?- Quantum field theory of evanescent photons in brain as quantum theory of consciousness. *Informatica* **1997**, *21*, 471–490.

38. Zheng, J.m.; Pollack, G.H. Long-range forces extending from polymer-gel surfaces. *Phys. Rev. E* **2003**, *68*, 031408. [CrossRef]

39. Del Giudice, E.; Voeikov, V.; Tedeschi, A.; Vitiello, G. The origin and the special role of coherent water in living systems. *Fields Cell* **2014**, 95–111. [CrossRef]

40. Renati, P.; Kovacs, Z.; De Ninno, A.; Tsenkova, R. Temperature dependence analysis of the NIR spectra of liquid water confirms the existence of two phases, one of which is in a coherent state. *J. Mol. Liq.* **2019**, *292*, 111449. [CrossRef]

41. Beggs, J.M.; Plenz, D. Neuronal avalanches in neocortical circuits. *J. Neurosci.* **2003**, *23*, 11167–11177. [CrossRef]

42. Bassett, D.S.; Meyer-Lindenberg, A.; Achard, S.; Duke, T.; Bullmore, E. Adaptive reconfiguration of fractal small-world human brain functional networks. *Proc. Natl. Acad. Sci. USA* **2006**, *103*, 19518–19523. [CrossRef]

43. Vitiello, G. Fractals, coherent states and self-similarity induced noncommutative geometry. *Phys. Lett. A* **2012**, *376*, 2527–2532. [CrossRef]

44. Vitiello, G. Fractals as macroscopic manifestation of squeezed coherent states and brain dynamics. *Proc. J. Phys. Conf. Ser.* **2012**, *380*, 012021. [CrossRef]

45. Stueckelberg, E.; Petermann, A. Normalization of constants in the quanta theory. *Helv. Phys. Acta* **1953**, *26*, 499.

46. Gell-Mann, M.; Low, F.E. Quantum electrodynamics at small distances. *Phys. Rev.* **1954**, *95*, 1300. [CrossRef]

47. Wilson, K.G.; Kogut, J. The renormalization group and the epsilon expansion. *Phys. Rep.* **1974**, *12*, 75–199. [CrossRef]

48. Collins, J.C. *Renormalization: An Introduction to Renormalization, the Renormalization Group and the Operator-Product Expansion*; Cambridge Monographs on Mathematical Physics; Cambridge University Press: Cambridge, UK, 1984. [CrossRef]

49. Peskin, M.E.; Schroeder, D.V. *An Introduction to Quantum Field Theory*; CRC Press: Boulder, CO, USA, 1995.

50. Cornwall, J.M.; Jackiw, R.; Tomboulis, E. Effective action for composite operators. *Phys. Rev. D* **1974**, *10*, 2428. [CrossRef]

51. Calzetta, E.; Hu, B.L. Nonequilibrium quantum fields: Closed-time-path effective action, Wigner function, and Boltzmann equation. *Phys. Rev. D* **1988**, *37*, 2878. [CrossRef]

52. Baym, G.; Kadanoff, L.P. Conservation laws and correlation functions. *Phys. Rev.* **1961**, *124*, 287. [CrossRef]

53. Baym, G. Self-consistent approximations in many-body systems. *Phys. Rev.* **1962**, *127*, 1391. [CrossRef]

54. Kadanoff, L.P.; Baym, G. *Quantum Statistical Mechanics: Green's Function Methods in Equilibrium Problems*; WA Benjamin: Los Angeles, CA, USA, 1962.

55. Berges, J. Introduction to nonequilibrium quantum field theory. In *AIP Conference Proceedings*; American Institute of Physics: College Park, MD, USA, 2004; Volume 739, pp. 3–62.

56. Juchem, S.; Cassing, W.; Greiner, C. Quantum dynamics and thermalization for out-of-equilibrium φ^4 theory. *Phys. Rev. D* **2004**, *69*, 025006. [CrossRef]

57. Busemeyer, J.R.; Wang, Z.; Townsend, J.T. Quantum dynamics of human decision-making. *J. Math. Psychol.* **2006**, *50*, 220–241. [CrossRef]

58. Pothos, E.M.; Busemeyer, J.R. A quantum probability explanation for violations of 'rational'decision theory. *Proc. R. Soc. B Biol. Sci.* **2009**, *276*, 2171–2178. [CrossRef]

59. Asano, M.; Basieva, I.; Khrennikov, A.; Ohya, M.; Tanaka, Y. Quantum-like generalization of the Bayesian updating scheme for objective and subjective mental uncertainties. *J. Math. Psychol.* **2012**, *56*, 166–175. [CrossRef]

60. Kvam, P.D.; Pleskac, T.J.; Yu, S.; Busemeyer, J.R. Interference effects of choice on confidence: Quantum characteristics of evidence accumulation. *Proc. Natl. Acad. Sci. USA* **2015**, *112*, 10645–10650. [CrossRef]
61. Bruza, P.D.; Wang, Z.; Busemeyer, J.R. Quantum cognition: A new theoretical approach to psychology. *Trends Cogn. Sci.* **2015**, *19*, 383–393. [CrossRef]
62. Tanaka, S.; Umegaki, T.; Nishiyama, A.; Kitoh-Nishioka, H. Dynamical free energy based model for quantum decision making. *Phys. A Stat. Mech. Its Appl.* **2022**, *605*, 127979. [CrossRef]